UC34c+d

LBL-16930
Preprint

Lawrence Berkeley Laboratory
UNIVERSITY OF CALIFORNIA

RECEIVED
LAWRENCE
BERKELEY LABORATORY

MAR 14 1984

LIBRARY AND
DOCUMENTS SECTION

Submitted to Physical Review C

TWO-PION CORRELATIONS IN HEAVY ION COLLISIONS

W.A. Zajc, J.A. Bistirlich, R.R. Bossingham,
H.R. Bowman, C.W. Clawson, K.M. Crowe, K.A. Frankel,
J.G. Ingersoll, J.M. Kurck, C.J. Martoff,
D.L. Murphy, J.O. Rasmussen, J.P. Sullivan, E. Yoo,
O. Hashimoto, M. Koike, W.J. McDonald, J.P. Miller,
and P. Truöl

January 1984

For Reference

Not to be taken from this room

LBL-16930
c.1

Prepared for the U.S. Department of Energy under Contract DE-AC03-76SF00098

DISCLAIMER

This document was prepared as an account of work sponsored by the United States Government. While this document is believed to contain correct information, neither the United States Government nor any agency thereof, nor the Regents of the University of California, nor any of their employees, makes any warranty, express or implied, or assumes any legal responsibility for the accuracy, completeness, or usefulness of any information, apparatus, product, or process disclosed, or represents that its use would not infringe privately owned rights. Reference herein to any specific commercial product, process, or service by its trade name, trademark, manufacturer, or otherwise, does not necessarily constitute or imply its endorsement, recommendation, or favoring by the United States Government or any agency thereof, or the Regents of the University of California. The views and opinions of authors expressed herein do not necessarily state or reflect those of the United States Government or any agency thereof or the Regents of the University of California.

To be submitted to Physical Review C
PACS #'s: 25.70Np, 25.70Bc
25.70Fg, 25.70Hi

LBL-16930

Two-Pion Correlations in Heavy Ion Collisions

W.A. Zajc, J.A. Bistirlich, R.R. Bossingham, H.R. Bowman, C.W. Clawson, K.M. Crowe, K.A. Frankel, J.G. Ingersoll, J.M. Kurck, C.J. Martoff, D.L. Murphy, J.O. Rasmussen, J.P. Sullivan, E. Yoo

Lawrence Berkeley Laboratory, University of California
Berkeley, CA 94720

O. Hashimoto, M. Koike

Institute for Nuclear Study, University of Tokyo
Tanashi, Tokyo 188, Japan

W.J. McDonald

University of Alberta, Edmonton, Alberta, Canada T6G 2J1

J.P. Miller

Boston University, Boston, MA 02215

P. Truöl

University of Zurich, 8001 Zurich, Switzerland

This work was supported by the Director, Office of Energy Research, Division of Nuclear Physics at the Office of High Energy and Nuclear Physics of the U.S. Department of Energy under Contract DE-AC03-76SF00098. Further support was provided by the INS-LBL collaboration program, Institute for Nuclear Study, University of Tokyo, JAPAN. We would also like to acknowledge the free computer time provided by D. Greiner of the HISS collaboration at LBL.

ABSTRACT

An application of intensity interferometry to relativistic heavy ion collisions is reported. The correlation between two like-charged pions is used to study the reactions Ar+KCl $\rightarrow 2\pi^{\pm} + X$ and Ne+NaF $\rightarrow 2\pi^{-} + X$, both at an incident beam energy of 1.8 A·GeV. Source sizes and lifetimes are measured and compared to the predictions of simple geometric models and of Monte Carlo cascade calculations. There appears to be a substantial coherent component of the pion source, although measurement is complicated by the presence of final state interactions.

A detailed discussion of the techniques of intensity interferometry is also presented. The generation of uncorrelated background events is discussed, along with the influence of the correlation on the background and the prescription for its removal. The statistical errors in the background spectrum are examined and found to have non-trivial implications for the analysis. The effect of the mutual Coulomb repulsion of the two pions, and of the pion-nuclear Coulomb interaction, on the two-pion correlation function is analyzed. The impact parameter bias resulting from a two-pion trigger is calculated and found to be substantial. Finally, a simple model for the interpretation of Gaussian source parameters is presented and compared to the preditions of Monte Carlo cascade calculations.

KEYWORD ABSTRACT

NUCLEAR REACTIONS ^{40}Ar(KCl) E_{LAB} = 1.8 A·GeV. Measured $2\pi^{+}$ and $2\pi^{-}$ correlations. Interferometry analysis deduced size and coherence of pion emission source. Techniques of background generation, statistics, and Coulomb corrections in intensity interferometry discussed. Impact parameter bias estimated. Results compared to Monte Carlo cascade code.

I. INTRODUCTION

The collision of two nuclei at relativistic energies is an event of both considerable interest and considerable complexity. The interest arises from the high energy densities expected in the collision region. The complexity results from the large number of inelastic nucleon-nucleon collisions. To date, all efforts to understand such a system proceed through the construction of a model, rather than an exact solution of the underlying dynamics. In the past ten years, a large variety of models have been used in attempts to explain the systematics of relativistic heavy ion collisions (RHIC), with varying degrees of success. Similarly, experimental attempts to discriminate between various approaches have been frustrated by the ability of models with vastly different (and mutually inconsistent) assumptions to predict equally well the single-particle momentum spectra.

Two-particle inclusive measurements offer a more sensitive tool for understanding RHIC. In particular, the measurement of two-particle relative momentum distributions allows one to determine the collision geometry quite directly, by using the technique of intensity interferometry. In this paper, the results of such a measurement for Ar+KCl and Ne+NaF collisions at 1.8 A·GeV are reported. In Section II, a brief description of intensity interferometry is provided. The experimental apparatus is described in Section III. Data analysis procedures are discussed at some length in Section IV. Results are presented in Section V, with a summary and conclusion in Section VI. Three appendices discuss the question of impact parameter biases, the error analysis of the background spectrum, and the consequences of a simple geometric model for the pion production process in RHIC.

II. INTENSITY INTERFEROMETRY

Intensity interferometry uses the correlations between like particles induced by Fermi or Bose statistics to determine the space and time dimensions of the particle source. The method is quite general, first finding application to the measurement of stellar diameters in the pioneering work of Hanbury-Brown and Twiss[1]. Goldhaber, Goldhaber, Lee, and Pais[2] (GGLP) were the first to extend these methods to particle physics. By modifying the Fermi statistical model to include symmetrization between like particles, GGLP were able to explain the observed differences in opening angles between like-charged pairs and oppositely-charged pairs of pions created in $p\bar{p}$ annihilation. Since then, many authors[3] have used similar approaches to measure the size of hadronic interaction regions. A particularly convenient approach to intensity interferometry in particle physics proceeds through the introduction of the two-particle correlation function C_2, first introduced by Kopylov and Podgoretskii[4]. An heuristic discussion is presented here for the sake of completeness. For further details, with particular emphasis on RHIC, the reader is referred to the work of Gyulassy et al.[5] and Yano and Koonin[6].

Consider the detection of two like pions, shown schematically in Figure 1. Assume that the pions are created in the same event, such that a pion of momentum p_1 is detected at x_1, while the pion detected at x_2 has momentum p_2. (In what follows, the quantities p, r, and x are four-vectors.) If the pion source extends over some spatial region including r_1 and r_2, there are two ways to obtain the same final state observed at x_1 and x_2. Since the particles are indistinguishable, the amplitudes for the two alternate paths must be added. The probability of such an event is then

proportional to the square of the resulting amplitude, so that (assuming the pions may be described by plane waves)

$$dP_{12} \sim \left| e^{ip_1(x_1-r_1)} e^{ip_2(x_2-r_2)} + e^{ip_1(x_1-r_2)} e^{ip_2(x_2-r_1)} \right|^2 dr_1 dr_2 \qquad (1)$$

If the distribution of individual pion sources in space and time is described by a distribution function $\rho(r)$, and if the emission of pions at different space-time points may be treated as statistically independent, the net probability is then obtained by integrating Eq. 1 over the coordinates r_1 and r_2, so that

$$P_{12} \sim \int dP_{12} \rho(r_1)\rho(r_2) = 1 + |\tilde{\rho}(q)|^2 \qquad (2)$$

where $q = p_2 - p_1$ and $\tilde{\rho}$ is the Fourier transform of $\rho(r)$ with respect to q. This is the essential result of intensity interferometry: The probability of detecting two bosons depends on their relative momentum, with an enhancement equal to the square of the Fourier transform of the source distribution function. If R is some characteristic source size, the range of the enhancement will extend over $q \sim 1/R$, as expected from the uncertainty principle. Thus, a comparison of the observed relative momentum spectrum to the relative momentum spectrum expected in the absence of Bose-Einstein correlations (using, for example, pion pairs from sources widely separated in space and time) permits extraction of the pion source size and lifetime.

The more refined treatments of Ref. 5 and 6 show that the LHS of Eq.2 may be expressed as the ratio of the two-particle inclusive cross section to the product of the single-particle cross sections (suitably normalized by the mean multiplicities), so that

$$P_{12} \equiv C_2(p_2,p_1) = \frac{\langle n_\pi \rangle^2}{\langle n_\pi(n_\pi-1)\rangle} \frac{\sigma_\pi \dfrac{d^6\sigma_\pi}{d^3p_1 d^3p_2}}{\dfrac{d^3\sigma_\pi}{dp_1{}^3} \cdot \dfrac{d^3\sigma_\pi}{dp_2{}^3}} \tag{3}$$

The above expression defines the two-particle correlation function C_2, which is generally a function of the two momenta p_1 and p_2. If the pions may be described by plane waves, and if the individual pion emitters may be regarded as point-like[7], then C_2 becomes a function of only the relative four-momentum q. Arguments similar to those leading to Eq. 2 then give for C_2

$$C_2(p_1,p_2) \rightarrow C_2(q) = 1 + |\tilde{\rho}(\vec{q},q_o)|^2$$

where $\vec{q} = \vec{p}_2-\vec{p}_1$ and $q_o = |E_2-E_1|$.

Note that the normalization of $\rho(r)$ insures that $|\rho(\vec{q}=0, q_o=0|^2 = 1$, so that an ideal $C_2(\vec{q},q_o)$ would have an intercept of 2.

As an example of this procedure, consider a source density given by

$$\rho(\vec{r},t) = \frac{1}{\pi^2R^3\tau} e^{-\frac{r^2}{R^2} - \frac{t^2}{\tau^2}} \tag{4}$$

where $R(\tau)$ is the distribution of pion emission points in space(time). Calculation of the squared Fourier transform for this distribution then gives for the correlation function

$$C_2(\vec{q},q_o) = 1 + \lambda e^{-\frac{1}{2}|\vec{q}|^2R^2 - \frac{1}{2}q_o{}^2\tau^2} \tag{5}$$

As noted above, the normalization of $\rho(r)$ would imply that $C_2(\vec{q}=q_o=0) = 2$. In practice, the zero-intercept of C_2 is usually observed to be somewhat less than 2. This observation motivated Deutschmann et al.[8] to introduce

the parameter λ to avoid the introduction of systematic biases in fitting the data to the observed correlation functions. Possible sources of the deviation of λ from unity and their interpretation will be discussed in Section V.

III. EXPERIMENTAL METHODS

Figure 2 shows a plan view of the apparatus used in this experiment. Beams of 1.8 A·GeV ^{40}Ar and ^{20}Ne from the Berkeley Bevalac were directed onto KCl and NaF targets, respectively, which in each case provides a nearly symmetric target-projectile system. Targets of 0.5 to 1.0 gm cm^{-2}, which provide an interaction probability on the order of 1%, gave a good compromise between high event rates and multiple scattering of the pions in the target material. Intensities were typically 10^8-10^9 beam particles per pulse, where one pulse is slightly less than a second in duration. At these intensitites, between .1 and 1 good events per pulse were obtained. (The Bevalac duty cycle is one pulse every six seconds at a magnetic field corresponding to 1.8 A·GeV).

Pions emerging at 45 ± 8 degrees from the beam direction were accepted into a simple magnetic spectrometer system. A 9 kG central field was provided by an H-type magnet with a 56cm x 168cm pole tip and a 21.5cm gap. The ingoing trajectories of the pions were defined by two small (30.2cm x 14.2cm) multi-wire proportional counters, MWPC1 and MWPC2. After being bent in the field, the pions pass through two large (200cm x 25cm) MWPCs, thereby defining their outgoing trajectories, and hence the bend angle. Each of the four MWPCs consisted of three planes of sense wires with 2mm wire spacing, with 1.4cm spacing between the sense planes.

A two-pion trigger is created using the scintillation counters S1, S2, various combinations of the A and B counters, and a fast signal FO from the MWPCs. The geometric overlap of a given A counter with a B counter defines 17 allowed combinations $(AB)_k$. Two-pion events are therefore defined by the requirement EVENT = $S1 \cdot S2 \cdot FO \cdot (AB)_m \cdot (AB)_n$, with $m \neq n$. Time-of-flight (TOF) signals were measured between S2 and the various AB combinations. The pulse height (ADC) for each A and B counter is also recorded. Proton contamination is reduced on-line by narrow TOF gate-widths, and off-line by a combination of further TOF cuts and ADC cuts (see Figure 3 for an example of typical TOF and ADC spectra). This procedure reduces the proton contamination to less than 1%, as may be seen in Figure 4. Note that the arrow at E_{cm} = 500 MeV in Figure 4a is equivalent to the arrow in Figure 4b located at $|\vec{p}_{lab}|$ = 700 MeV/c, so that the apparently large proton contamination in the first graph is in reality barely discernible in the total event sample. The narrow TOF gates also serve to reduce the electron contamination to a negligible level for all pion momenta considered here. Accidental triggers due to the simultaneous detection of two single-pion events are minimized by the narrow (< 100 ns) gate used in the overall trigger. Such events never exceeded a 5% contribution at the highest beam intensities and were reduced to a negligible level off-line using the time-of-flight data for each AB combination. More detailed information concerning the fast electronics and data acquisition, as well as the anlaysis codes to be described below, may be found elsewhere[9].

Off-line analysis begins by identifying all possible track candidates using a simple geometric algorithm. These candidates are then

momentum-analyzed using an interpolation method based on a Chebyshev parametrization of Monte Carlo tracks[10]. The accuracy of this procedure may be assessed from the contents of Table 1, which give the predicted resolution for the momentum, both in magnitude and in angle, as well as the intial position of each pion on the target (in the plane perpendicular to the beam). These results are calculated by a Monte Carlo procedure which includes the effects of the spatial extent of the beam on the target, the decay in flight of the pions, spatial resolution of the wire chambers, and multiple scattering and energy loss in the target, counters, MWPC's and air, averaged over the observed momentum spectrum. In Figure 5 the absolute and relative momentum resolution are shown as a function of the laboratory momentum. For low momenta, the resolution is determined by multiple scattering in the target and the 'S' counters, while for high momenta the spatial resolution (1mm) of the MWPC's in the bend plane is the limiting factor. For $|\vec{p}| >$ 200 MeV/c, the relative momentum resolution is always better than 2.5%. All results reported here will be for pions with laboratory momentum satisfying 220 MeV/c $< |\vec{p}_{lab}| <$ 800 MeV/c. These cuts provide an essentially proton-free sample of pions with high momentum resolution.

Of particular importance for an intensity interferometry experiment is the resolution in relative momentum. These distributions are shown in Figure 6, for both the relative momentum and the relative energy, again averaged over the single-pion momentum distribution. Also shown is the relative invariant mometum, $q_{inv} = (|q|^2 - q_o^2)^{1/2}$. This quantity will be used in the Coulomb corrections to the relative momentum spectrum, to be discussed below.

IV. GENERATION OF THE CORRELATION FUNCTION

Following the Chebyshev parametrization for the vector momentum of each track, cuts are made on various quality-of-fit variables, the TOF and pulse-height in the AB counters, etc. The result is a data set consisting of momentum-analyzed pion pairs, from which the correlation function will be created. This section describes the means by which C_2 is calculated and the motivation for doing so.

In principle the definition of C_2 as the ratio of the invariant cross sections (Eq. 3) could be used to calculate the correlation function. While this approach is often used in theoretical work[5], it is extremely impractical from an experimental point of view. Aside from the purely statistical problems resulting from binning events in six-dimensional phase-space, a more fundamental difficulty in triggered experiments is the bias introduced by the two-particle requirement. Unless the single-particle inclusive cross-sections in Eq. 3 reflect this bias, the numerator will contain pions from a different class of events than the denominator, which is known to produce spurious effects in the calculation of the correlation function[11]. Appendix A shows that such a bias does indeed exist for the two-pion trigger used in this experiment. By relating the number of produced pions to the number of participant nucleons, it is shown there that requiring pion production reduces the mean impact parameter $\langle b \rangle$ considerably from the unbiased value of 5.5fm (for Ar+KCl collisions). Not suprisingly, higher pion multiplicities are associated with smaller impact parameters, so that for the one-pion trigger (in our spectrometer) we have $\langle b(1\pi) \rangle = 3.3$fm, while for the two-pion trigger $\langle b(2\pi) \rangle = 1.2$fm.

To avoid the difficulties that arise from mixing pions from different event classes, an alternative approach based solely on the observed

two-particle relative momentum spectrum $A(q,q_o)$ is desirable. (For the remainder of this paper we will use q to denote $|\vec{q}|$). If a background spectrum $B(q,q_o)$ could be found such that all details such as production dynamics, experimental acceptances and biases, etc., were incorporated, EXCEPT those induced by Bose-Einstein correlations, then it is clear that C_2 would be given by

$$C_2(q,q_o) = \frac{A(q,q_o)}{B(q,q_o)} \tag{6}$$

The most common prescription used to generate $B(q,q_o)$ is that of different-event mixing, as first suggested by Kopylov[12]. In this scheme, fake events, generated by combining individual pions taken from different events, are used to calculate a "random" background spectrum in q and q_o. Intuitively, it would appear that acceptance effects, single-particle spectra, etc., would be contained in this spectrum, but that interference effects, which are not expected to extend to pions from different events, would be removed, thereby satisfying the definition of a suitable background spectrum.

In practice, it is found that different-event mixing never fully removes the correlations induced by Bose statistics. This is most easily appreciated by considering a hypothetical experiment that measures only a very small region of the total p_1~p_2 phase space. As the size of this region shrinks to zero, every real pion pair will be within the "range" of the correlation, so that p_1~p_2 for all events, and thus any mixing process on this data set will also create events with p_1~p_2. Mathematically, this may be understood by the following argument: First, we adopt the notation $C_2(p_1,p_2) = 1 + \Lambda\ (p_1,p_2)$. Eq. 3 may then be written in the schematic form

$$\frac{dn}{dp_1 dp_2} = \{1 + \Lambda(p_1,p_2)\} \frac{dn}{dp_1} \frac{dn}{dp_2} \tag{7}$$

The background spectrum generated by different-event mixing then has a distribution in p_1 given by integrating over all p_2, so that

$$\frac{dn_B}{dp_1} = \int_\Omega \frac{dn}{dp_1 dp_2} dp_2 = \frac{dn}{dp_1} \int_\Omega \{1 + \Lambda(p_1,p_2)\} \frac{dn}{dp_2} dp_2$$

$$\equiv \frac{dn}{dp_1} \{1 + \Delta(p_1;\Lambda)\} \tag{8}$$

In the above expression, Ω is the region of integration, which of course is given by the acceptance of the spectrometer used to measure the two-pion distribution. The desired single-particle spectrum dn/dp_1 is thus modified by a correction term $\Delta(p_1,\Lambda)$, which in the ideal case should be a quantity small compared to one. Similarly, a correlation function using this background spectrum will contain these (momentum-dependent) correction terms:

$$C_2^B (p_1,p_2) = \frac{1 + \Lambda(p_1,p_2)}{\{1 + \Delta(p_1;\Lambda)\}\{1 + \Delta(p_2;\Lambda)\}} \tag{9}$$

Before discussing the removal of the Δ's from the different-event mixing correlation function, several remarks are in order. First, it should be obvious that the above results are independent of the origin of the two-particle correlations. Instead, they derive immediately from the assumed form of Eq. 7, and therefore apply to any attempt to generate correlation functions, whether the source of the correlations is kinematic, dynamic, or statistical. Second, even in the limit of 4π spectrometer acceptance, the Δ's are non-zero. Explicit calculation of the Δ's, using reasonable forms for $\Lambda(q,q_o)$ and dn/dp_1, shows that the

correction terms in C_2 are of order $(\langle k_\pi \rangle R)^{-3}$, where $\langle k_\pi \rangle$ is the average pion momentum, and R is the pion source size. Very general arguments[5] independent of the assumed form for Λ and dn/dp_1, lead to the same conclusions. Thus, for $\Omega = 4\pi$ and for RHIC, these correction terms are of the order 2-5%. Finally, it should be clear that a "figure-of-merit" for the different-event mixing method is the average value of Δ over the data set. Since failure to remove these effects can lead to spurious conclusions concerning the degree of pion source coherence, large average values of $\Delta(>10\%)$ must be removed explicitly. We now direct our attention to the removal method.

Assume one had a priori knowledge of C_2, and thus of $\Lambda(q,q_o)$. Consider an arbitrary background event b_{ij} generated by taking a pion with momentum p_i from one event and one with momentum p_j from a different event. If each b_{ij} is assigned a weight given by

$$\omega(b_{ij}) \equiv \{1 + \Delta(p_i;\Lambda)\}\cdot\{1 + \Delta(p_j;\Lambda)\} \tag{10}$$

these weight factors will then precisely cancel the unwanted terms appearing in Eq. 9. Binning in terms of q and q_o simply introduces a sum over a projection operator $P\{(qq_o) \leftarrow (p_i p_j)\}$

$$\omega(q,q_o) = \sum_{ij} P\{(qq_o) \leftarrow (p_i p_j)\}\omega(b_{ij}) \tag{11}$$

without affecting the basic result that explicit knowledge of C_2 allows us to develop a prescription for weighting background events such that the spurious factors terms in Eq. 9 are cancelled.

In practice, of course, C_2 is not known beforehand. Instead, an interative procedure must be used. C_2 is parametrized in terms of assumed values for the source radius and lifetime. A weighted background spectrum

is calculated via Eq. 11, which is then used in Eq. 6 to calculate a new C_2. This correlation function is then fit to determine the new source parameters, which are then used to recalculate $B(q,q_o)$, and thus close the loop. Monte Carlo simulations of this procedure have verified that it does indeed regenerate the correlation function from pion pairs observed in a small acceptance region. The iteration converges to stable values for the radius and lifetime very quickly (between 2 and 4 iterations), and is independent of the starting values of these parameters (within reasonable limits, so that the first guess for the correlation function has some structure on the same scale as that observed in the data).

At each step of the iterative process, the correlation function is fit to the functional form of Eq. 4. Fits were performed using a maximum likelihood procedure to predict the actual number of observed pairs in a given $q-q_o$ bin in terms of $B(q,q_o)$ and the assumed form for C_2. Essential to this method is the assumption that the statistical errors in $B(q,q_o)$ are small compared to those in the real events. A naive extension of the sum in Eq. 11 to all $i \neq j$ would seemingly lead to a very large number of background events, thereby easily satisfying the criteria of negligible error in the determination of $B(q,q_o)$. In reality, the question of the statistical errors in the background spectrum is somewhat more subtle, and leads to the surprising conclusion that (if all possible background candidates are generated) the statistical fluctuation in a bin containing n background events is proportional to $n^{3/4}$, not $n^{1/2}$. The origins and implications of this behavior are discussed in Appendix B.

V. EXPERIMENTAL RESULTS

Results from three data sets are reported here, all for incident beam energies of 1.8 A·GeV. For the Ar+KCl system, approximately 6700 $2\pi^-$ pairs and 5500 $2\pi^+$ pairs passed all cuts. In the case of Ne+NaF, nearly 10,000 $2\pi^-$ pairs were accepted. All pions were required to have a laboratory momentum satisfying $220 < |\vec{p}| < 800$ MeV/c. Relative momentum and energy were always calculated in the nucleon-nucleon center-of-mass system. For relativistic pions, our laboratory acceptance of 45 ± 8 degrees translates to roughly 89 ± 12 degrees in the center-of-mass system. All three data sets were fit[13] to the functional form of Eq. 5; the results of which may be found in Table 2.

Before analyzing the results of the fitting procedure, we first discuss the visual presentation of the data. Figure 7 shows the appearance of an ideal $C_2(q,q_o)$ (as defined by Eq. 5 with λ equal to one) convoluted with our spectrometer's acceptance. The contours are separated by 10 MeV, and values of R and τ characteristic of nuclear dimensions are assumed. It is clear that only a limited region of the relative phase-space is accessible, dominated by events with $q \sim q_o$. (Note, however, that only half of the q-q_o plane is kinematically allowed, as calculation of the invariant relative momentum q_{inv} in the π-π center-of-mass shows that one always has $q > q_o$.) One consequence of our acceptance is that fixing q_o restricts q to a narrow band, so that a slice of the correlation function given by $C_2(q,q_o = \text{constant})$ is of little interest. Instead, we define the projections

$$\langle C_2(q)\rangle = \frac{\sum_{q_o} A(q,q_o)}{\sum_{q_o} B(q,q_o)} \tag{12}$$

and

$$\langle C_2(q_o)\rangle = \frac{\sum_{q} A(q,q_o)}{\sum_{q} B(q,q_o)}$$

where A and B are as defined in Eq. 6. We will always write these projections with brackets to emphasize that they are spectrometer-dependent observables. Nonetheless, they provide an adequate means for displaying the data and assessing quality of fits to the same. For convenience, the quantities defined in Eq. 12 will often be referred to as correlation functions, while keeping in mind that they are in reality projections of correlation functions.

A. GAMOW CORRECTIONS.

We first turn our attention to the entries labeled as "No Gamow." The corresponding correlation functions are shown in Figure 8. For both sets of $2\pi^-$ data, the radius is fit to a value of zero, and for all three systems the value of λ is less than 0.50, a substantial reduction from the expected value (for a fully random source) of 1.0.

This behavior is consistent with a systematic effect that has been neglected until this point: the mutual Coulomb interaction of the two pions. It is well known that the Coulomb interaction of two like-charged particles modifies the phase space density in relative momentum via the Gamow factor, so that

$$\frac{(d^3n/dq^3)_{\text{charged}}}{(d^3n/dq^3)_{\text{uncharged}}} \equiv G(\eta) = \frac{2\pi\eta}{e^{2\pi\eta}-1}\ , \quad \eta = \frac{me^2}{\hbar q} \tag{13}$$

(The corrections to this form due to the finite extent of the pion source have been calculated and found to be small[9].) Here e and m are the charge and reduced mass of the particles. This factor suppresses the probability of finding two like-charged particles with small relative velocities $\beta_{rel} \sim 1/137$. Note that β_{rel} must be calculated in the center-of-mass frame of the two pions, where, of course, one has $\beta_{rel} = q/m$. Substituting the previously defined relativistic invariant q_{inv} for q in the above expression gives the correct generalization to an arbitrary Lorentz frame, since in the center-of-mass frame of the two pions one has by definition $q_o = 0$. This observation is of more than passing interest, since it implies that the Gamow corrections are large, not just for small q, but rather along the entire $q = q_o$ line (see Figure 7).

Monte Carlo calculations have verified that large Gamow corrections persist in the two-pion relative momentum spectra as measured by our spectrometer, precisely because the good momentum resolution of this device enables us to resolve the region of suppression[14]. Since the net effect of the two-pion Coulomb interaction is to modify the correlation function $C_2(q,q_o) \rightarrow G(me^2/hq_{inv})C_2(q,q_o)$, it is important that the Gamow correction be applied to the background events via Eq. 10, rather than attempting to correct for its influence after the generation of C_2. These results are presented in Table 2 under the heading "Gamow corrected". The corresponding correlation functions are shown in Figure 9. In each case the radius now acquires a non-zero value and λ increases to the range 0.6-0.7.

B. INTERPRETATION OF R AND τ.

We now discuss the quantitative values obtained for R and τ in the context of the simple model for pion production presented in Appendix C.

There it is shown that: 1.) A radius R defined for a Gaussian source as in Eq. 4 is essentially indistinguishable (via intensity interferometry) from a source with uniform density of radius $R_u = 1.52R$. 2.) A schematic model for pion production gives

$$R = 0.56A^{1/3}\text{fm} \qquad \tau = 0.57A^{1/3}\text{fm}$$

where A is the mass number of one of the incident nuclei. (We use here units with c=1, so that lifetimes may be quoted in fm.) 3.) More realistic Monte Carlo cascade calculations[15] predict values of τ 2-3 times larger than the naive value given immediately above, but provide values of R consistent with the above estimate.

To facilitate comparison of our results to these predictions, we have combined the results of the various data sets using an $A^{1/3}$ parametrization to obtain

$$R = (1.0 \pm 0.2)A^{1/3}\text{fm} \qquad \tau = (0.8 \pm 0.3)A^{1/3}\text{fm}$$

The experimental value for τ obtained by this method is intermediate in value between the prediction of the geometric model and that of the cascade code. On the other hand, the measured value of R is substantially larger than either the geometric model or cascade calculations would indicate.

Before assessing the significance of the disagreement between these models and the data, it is necessary to examine more closely the errors in the determination of R and τ. Figure 10 displays the 68% and 95% confidence limits for R and τ allowed by each data set. It is clear that our maximum sensitivity is to some overall measure of the space-time extent (such as $R^2 + \tau^2$). This is simply the spatial consequence of our acceptance

in momentum space (where most pions have $q \simeq q_o$). Another consequence of the R-τ correlation is that specifying one of the parameters allows the other to be determined with significantly greater accuracy. Table 2 presents the results of fitting with either R or τ fixed to the "expected" value given by the schematic model. Of some interest are the cases where R has been fixed to the nominal value (as given by either the schematic model or the cascade codes) of $R = 0.56A^{1/3}$. Doing so always leads to values of τ larger than the prediction of the geometrical overlap model by a factor of 2-3, but in good agreement with the results of the cascade code calculations.

The most severe constraints on models of the pion source may be obtained by examining the confidence levels that result from using an assumed $A^{1/3}$ scaling behavior to combine the three data sets. These levels are presented in Fig. 11, where it is apparent that the 2σ errors in R and τ are substantially less than twice the 1σ errors in these quantities. (It is important to note that the 1σ errors quoted above have been obtained directly from the 68% confidence level, rather than by calculating the weighted average of the three sets of R and τ values.) Figure 11 clearly demonstrates that both the schematic model and the cascade codes predict a radius significantly smaller than our measured value. Conversely, both models predict values for the lifetime parameter consistent with our results.

C. EXTERNAL COULOMB CORRECTIONS.

There is an additional Coulomb interaction to be considered, that between a pion and all the nuclear protons. We call these the "Coulomb" interactions in contrast to the π-π interactions denoted by "Gamow"

interactions. Noticeable in Fig. 10 is the qualitative difference in the confidence level contours between the $2\pi^-$ and $2\pi^+$ measurements. We have attempted to determine if these differences are due to the opposite sign of the Coulomb interactions experienced by the π^-'s with the nuclear charge as compared to the π^+'s. Using a first-order formalism correct in both the classical and quantum mechanical limit[16] the momentum shift of each pion due to the Coulomb interaction with a nuclear fragment of charge Z_i and four-velocity u_i is calculated in terms of the final pion momentum according to

$$\delta p_\mu(p_f) = \frac{Z_i}{137}[(p_f)_\mu - (p_f u_i)u_{i\mu}] \frac{(p_f u_i)R_{eff}}{1+[(p_f u_i)^2 - m_\pi^2]R_{eff}^2} \tag{14}$$

The effective radius R_{eff} is the reciprocal of the mean inverse radius

$$R_{eff} = \left\langle \frac{1}{r} \right\rangle^{-1} = \frac{\sqrt{\pi}}{2} R$$

where the last equality holds for our usual Gaussian source parametrization. We have idealized the complicated final-state distribution of nuclear charge by three charge fragments, two having charge $(1-f)Z$ and moving with the projectile or target velocity, and the third having charge $f \cdot 2Z$ at rest in the center-of-mass, where Z is the charge of one of the incident nuclei. Guided by the results for mean impact parameter biases presented in Appendix A, we have chosen $f = 0.80$. Eq. 14 is used to correct the momentum of each observed pion; then the correlation function is calculated in the usual fashion. These results appear in Table 2 with the designation "Gamow and Coulomb corrected". In all cases the changes in extracted parameters are much smaller than the statistical errors, which is in accord with our intuitive expectations that the changes in the relative momentum

spectrum will be small, since each pion receives essentially the same impulse. In reality, such a post hoc correction procedure is at best a crude approximation to the very complicated multi-body Coulomb problem, but the large kinetic energies of the pions relative to their potential energies lead us to conclude that any such effects are likely to be small.

D. IMPLICATIONS FOR SOURCE COHERENCE.

We now discuss briefly the significance of the values obtained for λ in Table 2. Many authors have cited deviations of this parameter from unity as evidence for coherence in the pion source, since for a maximally coherent source one has $\lambda = 0$. Furthermore, the assumption of a completely chaotic source leading to independent emission of pions is at best an approximation, since the relevant pion wavelengths are not substantially smaller than the inferred source dimensions[17]. Nonetheless, to date experimental complications prohibit any quantitative conclusions concerning the fraction of coherent emitters implied by a given value of λ. First note the direct coupling between the Gamow correction and the value obtained for λ. A second difficulty arises from the iterative generation of C_2 discussed in Section IV, which introduces a systematic tendency to increase the errors in λ from the purely statistical values quoted in Table 2. Other effects known to affect the value of λ, such as the creation of pions through the decay of long-lived resonances, or the averaging over unobserved reaction variables[11] further obscure the interpretation of deviations of this variable from unity in a given experiment, since a very complete set of measurements indeed would be required to determine which of these many contributions is the dominant one.

E. COMPARISON TO OTHER RESULTS.

We conclude this section with a comparison of our results to those obtained by other authors. At 1.8 A·GeV, the only two-pion experiments reported in the literature are for Ar nuclei incident on heavy (Pb_3O_4 or BaI_2) targets[18,19]. Rather than attempting to deal with the complicated issues of the role of impact parameter biases and spectator matter in asymmetric collisions, we concentrate on the only other result reported for the Ar+KCl system, at the slightly different energy of 1.5 A·GeV[20]. (This corresponds to a center-of-mass energy differing by less than 10% from ours.) These authors perform their fits by fixing the value of τ to 1.5 fm. The contours of Figure 10a allow us to read off the value of R obtained in our analysis when τ is fixed to 1.5 fm, viz. R = 3.6±0.40 fm, in excellent agreement with their value (for their data set most closely analogous to ours, i.e., the Gamow corrected analysis for pions with center-of-mass momentum greater than 150 Mev/c), of R = 4.14±0.51 fm. The value of λ measured for their Gamow corrected data, λ = 1.06±0.24, is statistically consistent with the value extracted in this experiment, although we note that these authors systematically find values of λ higher than those reported here. We offer no explanation of this phenomenon, other than to observe that the two experiments are more complementary than comparable, one being a high statistics, high resolution exploration of a narrow region of relative momentum, while the other provides a relatively unbiased global sample of events.

VI. CONCLUSIONS

We have shown that a high statistics intensity interferometry measurement of pion source parameters in RHIC provides valuable information for

dynamical models of these collisions. The two-pion trigger itself has been shown to give a significant bias towards central collisions. The effect of the two-pion relative Coulomb interaction has been analyzed and found to be important, while correction for the pion-nuclear Coulomb interaction produced little change in the extracted radius and lifetime. These final state interactions, and the iterative nature of the background generation, prevent any definite statement quantifying the coherent contribution to the pion source. The results presented here are consistent with previous measurements, and should provide a basis for future experiments using larger acceptance spectrometers to apply these techniques to heavier nuclear systems.

ACKNOWLEDGEMENTS

This work was supported by the Director, Office of Energy Research, Division of Nuclear Physics at the Office of High Energy and Nuclear Physics of the U.S. Department of Energy under Contract DE-AC03-76SF00098. Further support was provided by the INS-LBL collaboration program, Institute for Nuclear Study, University of Tokyo, JAPAN. We would also like to acknowledge the free computer time provided by D. Greiner of the HISS collaboration at LBL.

APPENDIX A: IMPACT PARAMETERS BIAS IN A TWO-PION TRIGGER

In this appendix we argue that a two-pion trigger provides a good approximation to a central collision trigger. We do so by using the observed correlation between pion multiplicity and participant nucleon multiplicity to establish the relation between pion multiplicity and impact parameter. Streamer chamber data are then used to relate the trigger requirement of this experiment to the total pion multiplicity, and thus to the mean impact parameter.

Figure 12 shows the mean negative pion multiplicity is linearly proportional to Q, the total number of participant protons, for 1.8 A·GeV Ar+KCl collisions[21]. The number of participant protons may be calculated as a function of impact parameter with an analytic approximation (for symmetric systems) due to Swiatecki[22]

$$Q(b) \cong 2Z(1 - \beta)^2[1 + \left(\frac{3}{\sqrt{2}} - 1\right)\beta] \qquad (A.1)$$

where $\beta = b/b_m$ and b_m is the maximum impact parameter 2R. The normalization is in terms of the total number of protons, so that $Q(b=0) = 2Z$.

The rough nature of these arguments justifies the further approximation (for small values of β):

$$\begin{aligned} Q(b) &= 2Z(1 - \beta)^2(1 + 1.12\beta) \\ &\simeq 2Z(1 - \beta) \end{aligned} \qquad (A.2)$$

This approximation is valid to (at worst) 20% for $\beta < 0.5$. In fact, evidence from recent Monte Carlo calculations (see Figure 8 in Cugnon and D. L' Hote[23]) favors this linear form over Eq. A.1 for 0.8 A·GeV/A collisions. Eq. A.2 allows us to translate Q directly into impact parameter; such a scale has been applied to the upper axis of Figure 12.

We now use streamer chamber data[24] to determine the mean pion multiplicity imposed by our two-pion trigger requirement. These data consist of approximately 3000 1.8 A·GeV Ar+KCl events taken with an inelastic trigger sensitive to approximately 85% of the total reaction cross section. All negative tracks in this sample have been momentum analyzed, which allows us to selectively examine those events satisfying the two-pion trigger used in this experiment. Figure 13 shows the pion multiplicity distribution which results from requiring two pions in our spectrometer acceptance. As shown by the curve, the distribution is roughly Poisson, with a mean given by $\langle n_\pi \rangle = 6.14 \pm 0.18$.

We can now use Figure 12 to immediately translate $\langle n_\pi \rangle$ into the equivalent Q, and thus the corresponding impact parameter, thereby obtaining $\langle b \rangle = 1.2$fm. Assuming the fluctuations in $\langle n_\pi \rangle$ are in fact Poisson, the fluctuation in $\langle b \rangle$ may be determined in a similar fashion to be 2.8fm. The fact that Figure 13 is somewhat narrower than the superimposed Poisson distribution (and the fact that negative impact parameters are meaningless, so that fluctuations of 2.8fm about 1.2fm must be asymmetric) indicate that this method provides an overestimate for the event-to-event fluctuations about $\langle b \rangle$.

APPENDIX B: BACKGROUND FLUCTUATIONS

In this appendix we examine the statistical fluctuations in a spectrum of background events generated by creating all possible combinations of pions taken from different events. In particular, we show that if such a process generates n events in a given bin, the statistical fluctuations of this quantity are of order $n^{3/4}$, not $n^{1/2}$. We begin by examining a schematic model that illustrates the basic principles involved[25].

Assume we wish to calculate the area of the small region Ω shown in Figure 14, using a straightforward Monte Carlo technique, Ordered pairs (n_x, n_y) would be thrown randomly over the area L^2, with the calculated area of Ω being proportional to the number m of such pairs contained within Ω. The error in this estimate will of course be proportional to $m^{1/2}$.

Now suppose we attempt to circumvent the requirement of generating M random pairs over the are L^2, and instead pick only N random points n_1 along the x axis, then use these SAME points along the y axis to define the set of points in the plane (n_i, n_j). This process generates N(N-1)/2 such pairs, but our intuition suggests that the statistical significance of such a set is still only of order $N^{1/2}$.

Simple error propagation suffices to confirm this suspicion. If $n_x = \ell_x N/L$ is the mean number along the x axis expected to fall in Ω, and similarly for n_y along the y axis, the number of "random" points in Ω is then $n = n_x n_y$. We now use standard methods to calculate the error in this quantity, thus

$$\sigma^2(n_\Omega) = \left(\frac{\partial n_\Omega}{\partial n_x}\right)^2 \sigma^2(n_x) + \left(\frac{\partial n_\Omega}{\partial n_y}\right)^2 \sigma^2(n_y)$$

$$= n_y^2 n_x + n_x^2 n_y$$

$$= n_\Omega[(\ell_x + \ell_y)\,\frac{N}{L}] \qquad \text{(B.1)}$$

Specializing to the case $\ell_x = \ell_y$, we immediately obtain from the above $\sigma(n_\Omega) = \sqrt{2}\, n_\Omega^{3/4}$. Had Ω been located on the diagonal of the region L^2, as for the region labeled Ω' in Figure 14, n_x and n_y are no longer even approximately independent, and we obtain instead $\sigma(n_\Omega) = 2\, n_\Omega^{3/4}$. The generalization to d dimensions is trivial and gives for the fluctuations

about the mean number n_v in a sub-volume V $\sigma(n_v) = d \cdot n_v^{(1-\frac{1}{2d})}$.

This model is suggestive of the different-event mixing prescription used to generate a background spectrum in intensity interferometry analyses: The N points chosen represent the N pion events, with the real events being distributed along the diagonal and the background events coming from the pairs (n_i, n_j), $i \neq j$. However, a typical correlation analysis involves a complicated projection from the six-dimensional $p_1 p_2$ space into a two-dimensional qq_o sub-space. Rather than attempting to extend our model (which really is intended only as a plausibility argument) to this case, we instead demonstrate empirically that the background fluctuations are proportional to $n^{3/4}$, corresponding to d = 2.

To do so, we define the variable Γ^2 given by

$$\Gamma^2 = \sum_{ij} \frac{(A_{ij} - B_{ij})^2}{\sigma^2(A_{ij}) + \sigma^2(B_{ij})} \tag{B.2}$$

where the sum over i and j represents a summation over the q and q_o bins in a relative momentum spectrum. Here B_{ij} is the number of background events in a given bin, and A_{ij} is some other distribution we expect to be identical with the B_{ij}'s in the limit of large statistics for A and B. The σ's are the assumed errors for each A and B. Since by definition Γ^2 has expectation value = 1, explicit evaluation of this variable for various assumed forms of the σ's allows us to determine the form best supported by the data. As our known A distribution we take the real two-pion events with $|q| > 150$ MeV/c, where all evidence (see Figure 9) indicates the absence of correlations. Similarly, the B distribution is taken to be the background spectrum in the same relative momentum interval. The functional dependence of $\sigma(B)$ is parametrized with the general d-dimensional result,

i.e., $\sigma(B) = d \cdot B^{1-\frac{1}{2d}}$. Testing two different data sets then gives p = 0.77±0.02 and p = 0.75±0.02, where p = 1 - 1/2d, thereby confirming the $n^{3/4}$ form for background fluctuations corresponding to d = 2. (See Ref. 9 for a discussion of the error estimates on p.)

Since the errors on n background events in a given bin are no longer Gaussian, the usual property of invariance of statistical significance under binning is lost. To see this, suppose we wish to create a background spectrum with negligible fluctuations in a given bin relative to the fluctuations in the number of real events expected in the same bin. Let the number of real events in the total sample be N, and assume the bin size is such that a fraction of them f fall into the i-th bin, so $n_i = fN$. Assume that the fraction of real events used to generate the background spectrum by different-event mixing is g, so that the total number of background events created is approximately $(gN)^2/2$. If we retain the notation C_2 for the correlation function, the expected number of background events in the i-th bin is then of course $m_i = \frac{f}{C_2} \cdot \frac{(gN)^2}{2}$. The correlation function as calculated for this bin is then n_i/m_i. Requiring that the errors in n_i dominate the error in the calculated correlation function then implies

$$\left(\frac{\sigma_m}{m}\right)^2 << \left(\frac{\sigma_n}{n}\right)^2$$

Using the above expressions for n_i and m_i, and assuming $\sigma_{m_i} = 2m_i^{3/4}$, we obtain the condition

$$\frac{1}{g}\sqrt{2C_2 f} << \frac{1}{4} \qquad \text{(B.3)}$$

While independent of the original number of events N, this result does depend both on g, the fraction used in the background generation and f, the fractional bin size. The fact that small background errors requires

g to be large is, of course, reasonable. Setting g = 1 then establishes the maximum allowed bin sizes

$$f \cdot C_2 << \frac{1}{32} \approx 3\% \tag{B.4}$$

Failure to satisfy this condition for each bin will invalidate the requirement of small background errors necessary to a Principle of Maximum Likelihood fitting procedure. This inequality is satisfied for nearly all of the bins used in generating the correlation functions calculated in this paper. We have verified that an alternative fitting method, based on minimization of a quantity that explicitly contains the background errors (the quantity Γ^2 defined in Eq. B.2), produces essentially the same source parameters as calculated by the Principle of Maximum Likelihood analysis.

APPENDIX C: GAUSSIAN MODELS FOR PION SOURCE PAREMETERS

This appendix explores some simple consequences of the Gaussian parametrization used for the pion source in this paper. We begin by interpreting R in terms of conventional nuclear radii:

The normalized Gaussian (spatial) distribution implied by Eq. 4 in the text is given by

$$\rho(\vec{r})d\vec{r} = \frac{1}{\pi^{3/2}R^3} e^{-r^2/R} d\vec{r} \tag{C.1}$$

To obtain the value of R equivalent to a uniform distribution R_u, we can equate moments of these distributions, thus obtaining

$$R = \frac{3\sqrt{\pi}}{8} R_u \cong \frac{R_u}{1.50}$$

by equating <r> for the two distributions, and

$$R = \sqrt{\frac{2}{5}}\, R_u \cong \frac{R_u}{1.58}$$

by equating $\langle r^2 \rangle$. These are but special cases of the general result stated by GGLP[2] that for $R = R_u/1.52$, the squared Fourier transform of a Gaussian distribution differs from the corresponding transform of the uniform distribution by 2% or less everywhere. Thus, no foreseeable intensity interferometry experiment can hope to distinguish between these two distributions.

To motivate the use of a Gaussian to describe the space-time distribution of pion sources, we use the following heuristic model for pion production in RHIC[26]: Consider the collision of two equal-mass nuclei at impact parameter b, in the center-of-mass frame, where each is moving with velocity $\pm\, \beta_{cm}$. Let the nucleon density for each nucleus be described by a Lorentz-contracted Gaussian of radius R_A.

$$\rho_{\pm}(r)dr = \frac{\gamma_{cm}}{\pi^{3/2} R_A^3}\, e^{-[x^2 + (y \pm \frac{b}{2})^2 + \gamma_{cm}^2 (z \pm \beta_{cm} t)^2]/R_A^2}\, dxdydz \qquad (C.2)$$

As discussed above, R_A is given in terms of the corresponding uniform-density radius R_u via $R_A/1.52 = 0.8 \cdot A^{1/3}$fm.

Assume the pion production rate is given by the overlap of these densities, so that

$$\frac{d^4 n_\pi}{dr^3 dt} = \rho_+(\vec{r})\rho_-(\vec{r}) \cdot \sigma_{NN} \cdot v_{rel} \qquad (C.3)$$

Here σ_{NN} is the NN cross section for pion production, and v_{rel} is the NN relative velocity. Ignoring all such effects as pion reabsorption, slowing of the incident nuclei, transverse expansion, etc., the pion source density may then be written as

$$\rho_\pi(\vec{r}t) \equiv \frac{d^4n_\pi}{dr^3dt} \sim e^{-\frac{2}{R_A^2}[x^2 + y^2 + \gamma_{cm}^2 z^2]} e^{-2\beta_{cm}^2\gamma_{cm}^2 t^2/R_A^2} e^{-b^2/2R_A^2}$$

Thus, the source is also Gaussian in space and time, with lifetime and (transverse) radius parameters given by

$$R = \frac{R_A}{\sqrt{2}} \qquad \tau = \frac{R_A}{\sqrt{2}\beta_{cm}\gamma_{cm}} \tag{C.4}$$

(Here we have absorbed the factor of two so that the source takes on the precise form assumed in Eq. 4 of the text.) The neglected effects mentioned above all tend to increase the values of R and τ, so that the above values should be regarded as lower limits. Using the $A^{1/3}$ parametrization of R_A introduced above, and specializing to the values of β_{cm} and γ_{cm} appropriate to 1.8 A·GeV beam energies, we have for R and τ:

$$R = 0.56A^{1/3}\text{fm} \qquad \tau = 0.57A^{1/3}\text{fm} \tag{C.5}$$

Note that the near-equivalence of the predicted values for R and τ is "accidental" in the sense that $\beta_{cm}\gamma_{cm}$ is very nearly equal to one for this particular beam energy. Also note that while the source strength depends on the impact parameter b, the source radius R does not. The parametrization for R in Eq. C.5 is in good agreement with the relation $R = 0.50 \cdot A^{1/3}$ found by Cugnon and Koonin[27] by fitting the results of Monte Carlo cascade code calculations of pion production sites. (This result differs by a factor of 2 from the result found in their paper, again due to writing their radius in the same form as Eq. 4 of this work.)

We may also apply the Gaussian form for the distribution of pion sources in time to the Monte Carlo cascade results of Cugnon et al[15], which provides a quantitative picture for the temporal as well as the spatial

evolution of a heavy ion collision. Figure 15 shows their results for the collision of two Ca nuclei at a beam energy of 1.8 A·GeV. Two curves are shown, one giving the production of free pions plus delta resonances, while the dotted curve gives the number of free pions as a function of time (deltas being regarded as "bound" pions). Maximum overlap occurs for ct = 5.1fm. The circular and triangle points are the results obtained by integrating

$$\frac{dN_o}{dt} = N_o \, e^{-t^2/\tau^2} \tag{C.6}$$

for appropriately chosen values of τ. Thus, for the $N_\pi + N_\Delta$ curve, we have for $t > 5.1$fm,

$$N(t) = \frac{1}{2}N(t = \infty)\left[1 + \mathrm{erf}\left(\frac{t-5.1}{\tau}\right)\right]$$

with $\tau = 2.31$fm. For the free pion production curve, we have $\tau = 5.55$fm.

These expressions provide reasonable approximations to the time dependence predicted by the Monte Carlo code, particularly for the total production rate (the closed circles). The required value of $\tau = 2.31$fm is in good agreement with that estimated by the schematic argument based on Gaussian overlap, i.e., $\tau > 1.95$fm. Note, however, that the production of free pions is predicted to proceed at a much slower rate, due to reabsorption, energy dependent cross sections and finite delta lifetimes. Nevertheless, the time development is still roughly described by the Gaussian parametrization.

Table 1		
Resolution for Fitted Quantities in Presence of Energy Loss and Multiple Scattering		
Quantity	$\langle$(actual-fit)$\rangle$	$\langle$(actual-fit)$^2\rangle$
$\lvert\vec{p}\rvert$ (MeV/c)	3.74	3.79
θ (degrees)	0.042	1.01
ϕ (degrees)	5.63×10^{-3}	1.39
x^{int} (cm.)	-0.053	1.09
y^{int} (cm.)	0.046	0.893

Table 2

System	Fit conditions	λ	R (fm)	ct (fm)	χ^2/NDF
Ar+KCl $2\pi^-$	No Gamow	0.40±.05	$0.0^{+1.1}_{-0.0}$	$4.58^{+0.4}_{-1.0}$	57.2/80
	Gamow corrected	0.63±.04	$2.88^{+0.5}_{-0.9}$	$3.29^{+1.4}_{-1.6}$	98.2/80
	Gamow corrected, R fixed	0.64±.04	1.92	$4.5^{+0.6}_{-0.4}$	98.2/80
	Gamow corrected, T fixed	0.64±.04	$3.50^{+.37}_{-.35}$	1.95	98.6/80
	Gamow and Coulomb corrected	0.63±.04	$2.77^{+.6}_{-.9}$	$3.44^{+1.1}_{-1.5}$	80.3/80
Ar+KCl $2\pi^+$	No Gamow	0.48±.07	2.26 1.4	$4.12^{+1.2}_{-2.0}$	52.4/81
	Gamow Corrected	0.73±.07	$4.20^{+.4}_{-.6}$	$1.54^{+2.4}_{-1.54}$	67.1/81
	Gamow corrected R fixed	0.69±.09	1.92	$5.5^{+0.9}_{-1.8}$	67.1/81
	Gamow corrected T fixed	0.72±.06	4.10±.54	1.95	67.2/81
	Gamow and Coulomb corrected	0.73±.07	4.10±0.4	$1.76^{+2.10}_{-1.76}$	78.5/81
Ne+NaF $2\pi^-$	No Gamow	0.46±.09	$0.0^{+3.1}_{-0.0}$	2.98±1.0	76.5/82
	Gamow corrected	0.59±.08	$1.83^{+.8}_{-1.6}$	$2.96^{+.90}_{-1.0}$	125.7/82
	Gamow corrected, R fixed	0.59±.06	1.52	3.3±0.3	126.1/82
	Gamow corrected, T fixed	0.60±.06	2.80±.30	1.54	126.6/82

REFERENCES

1. R. Hanbury Brown and R.Q. Twiss, Phil. Mag. 45, 663 (1954).

2. G. Goldhaber, S. Goldhaber, W. Lee, and A. Pais, Phys. Rev. 120, 300 (1960).

3. An extensive bibliography may be found in Ref. 8.

4. G.I. Kopylov and M. I. Podgoretskii, Sov. J. Nucl. Phys. 19, 215, and references contained therein, (1974).

5. M. Gyulassy, S.K. Kaufmann, and L.W. Wilson, Phys. Rev. C20, 2267 (1979).

6. F.B. Yano and S.E. Koonin, Phys. Lett. 78B, 556 (1978).

7. E.V. Shuryak, Sov. J. Nucl. Phys. 18, 667 (1974).

8. M. Deutschmann et al., CERN/EN/PHYS 78-1 (1978).

9. "Two-pion Correlations in Heavy Ion Collisions," William A. Zajc, LBL-14864, (unpublished). H. von Fellenburg (Thesis, University of Zurich, 1977).

10. H. Wind, Function Parametrization, in Proc. of 1972 CERN Computing and Data Processing School, CERN Report 72-21.

11. M. Gyulassy, Phys. Rev. Lett. 48, 454 (1982).

12. G.I. Kopylov, Phys. Lett. 50B, 472 (1974).

13. The values quoted in Table 2 for chi-squared per degree of freedom express the deviation of the correlation function from the form assumed in the fitting procedure, summed over all bins with more than 5 events in the real spectrum. This restriction is necessary so that chi-squared forms a valid statistic, see e.g., "Probability and Statistics in Particle Physics", A.G. Frodesen, O. Skjeggestad, and H. Tofte, Universitetsforlaget, Bergen p. 418ff. (1979). Note that the actual

fits were performed using the Principle of Maximum Likelihood, not chi-squared minimization.

14. For very small values of the relative momentum q(q < 15 MeV/c), the systematics of track recognition for pion pairs with small spatial separation are such that the calculated q tends to underestimate the actual value, leading to an overcorrection in the Gamow formulation. We have verified that this effect is restricted to the lowest two bins of the correlation function, and that exclusion of these bins in the fitting procedure does not affect the results presented in the text. For further details see Ref. 8.

15. J. Cugnon, D. Kinet, and J. Vandermeulen, Nucl. Phys. A379, 553 (1982).

16. M. Gyulassy and S.K. Kauffmann, Nucl. Phys. A362, 503 (1981).

17. R. Glauber, private communication.

18. S.Y. Fung et al., Phys. Rev. Lett. 41, 1592 (1978).

19. J.J. Lu et al., Phys. Rev. Lett. 46, 898 (1981).

20. D. Deavis et al., Phys. Rev. C 27, 910 (1983).

21. K.V. Bibber and A. Sandoval, in Heavy Ion Science, (Plenum Press, 1982).

22. As presented by L.S. Oliveira, University of California Ph.D Thesis, LBL-8561 (1978).

23. J. Cugnon and D. L'Hote, Nucl. Phys. A397, 519 (1983).

24. We would like to thank D. Beavis of the University of California, Riverside, for providing this data and for valuable conversations concerning its interpretation.

25. One of us (WAZ) wishes to acknowledge a valuable conversation with M. Gyulassy concerning this approach.

26. A. similar model was used by Libbrecht and Koonin (Phys. Rev. Lett. 43, 1581 (1979)) to analyze distortions in pion spectra resulting from the Coulomb interaction with the nuclear charge.

27. J. Cugnon and S.E. Koonin, Nucl. Phys. A355, 477 (1981).

FIGURE CAPTIONS

Fig. 1. Schematic illustration of a two-pion correlation experiment in which a pion of momentum p_1 is detected at x_1 simultaneously with the detection of a pion with momentum p_2 at x_2. The pions are assumed to originate from an extended source encompassing r_1 and r_2.

Fig. 2. Plan view of the experimental apparatus.

Fig. 3. a.) TOF spectrum for π's and protons. Each bin corresponds to 1.6ns. b.) ADC spectrum showing the pulse heights obtained for π's and protons.

Fig. 4. a.) Invariant single-particle spectrum (arbitrary normalization) for Ar+KCl $\rightarrow 2\pi^+ + X$ events. b.) Raw spectrum (uncorrected for spectrometer acceptance) in the laboratory for the same reaction as above. The arrow at E_{cm} = 500 MeV in (a) is equivalent to the arrow in (b) at $|\vec{p}_{lab}|$ = 700 MeV/c.

Fig. 5 Relative (a) and absolute (b) momentum resolution as a function of the magnitude of the laboratory momentum.

Fig. 6. a.) Resolution in the magnitude of the relative momentum as a function of the relative momentum. b.) Resolution in the relative energy as a function of the relative energy. c.) Resolution in the magnitude of the relative four-momentum, as a function of the relative three-momentum.

Fig. 7. Profiles of a theoretical correlation function with nuclear dimensions evaluated over the spectrometer acceptance used in this experiment. The region on the left-hand-side of the ridge is kinematically forbidden.

Fig. 8. Projected correlation functions with no Gamow correction for the systems a.) Ar+KCl → $2\pi^-$ + X b.) Ar+KCl → $2\pi^+$ + X c.) Ne+NaF → $2\pi^-$ + X.

Fig. 9. Projected correlation functions after Gamow correction for the systems a.) Ar+KCl → $2\pi^-$ + X b.) Ar+KCl → $2\pi^+$ + X c.) Ne+NaF → $2\pi^-$ + X.

Fig. 10. Contours for the 68% and 95% confidence levels arising from fits to Eq. 10 in the text. a.) Ar+KCl → $2\pi^-$ + X b.) Ar+KCl → $2\pi^+$ + X c.) Ne+NaF → $2\pi^-$ + X.

Fig. 11. Contours of the 68% and 95% confidence levels from combining the three data sets in Fig. 10 using an $A^{1/3}$ scaling between ^{40}Ar and ^{20}Ne results.

Fig. 12. Relation between total charge multiplicity and mean pion multiplicity $\langle M_\pi(Q)\rangle$. Also shown is a schematic impact parameter scale.

Fig. 13. Total pion multiplicity distribution for those events in 1.8 A·GeV Ar+KCl collisions satisfying the two-pion trigger requirement used in this experiment.

Fig. 14. Schematic illustration of Monte Carlo area calculations analogous to two-pion background event generation.

Fig. 15. The curves are Monte Carlo calculations from Ref. 15 of production rates for pions and deltas from 1.8 A·GeV Ca+Ca collisions. The points are predictions assuming a Gaussian dependence in time.

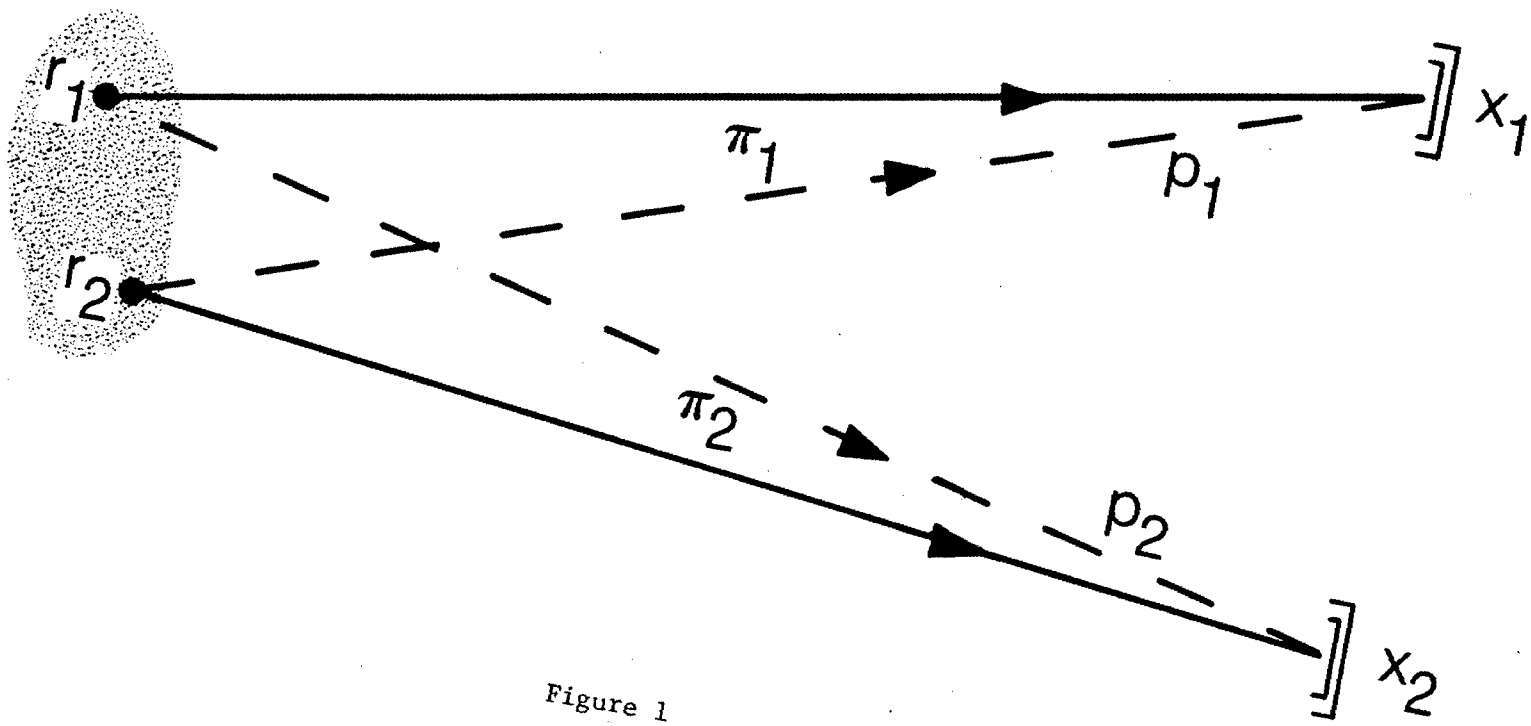

Figure 1

XBL 815-9836

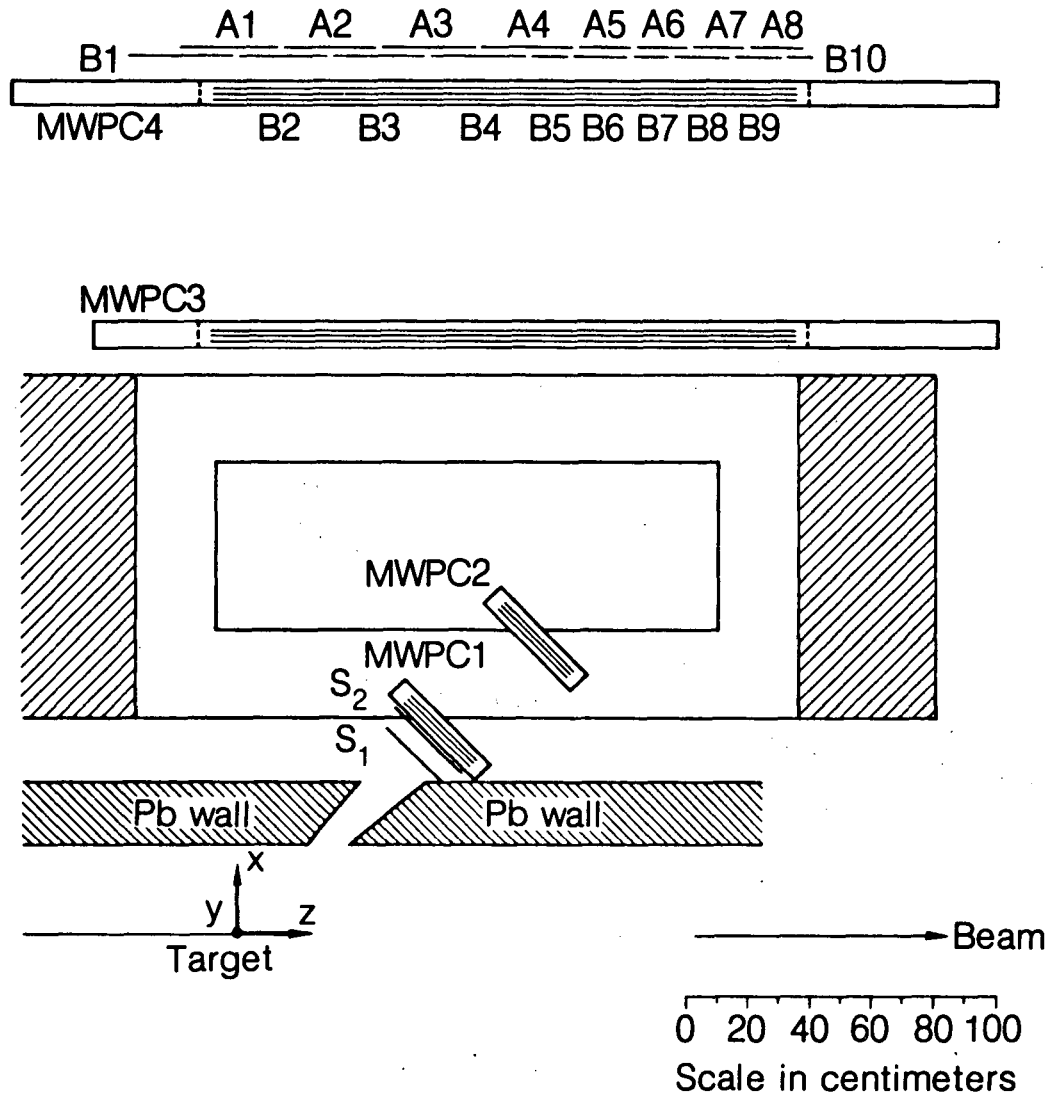

XBL 8312-7456

Figure 2

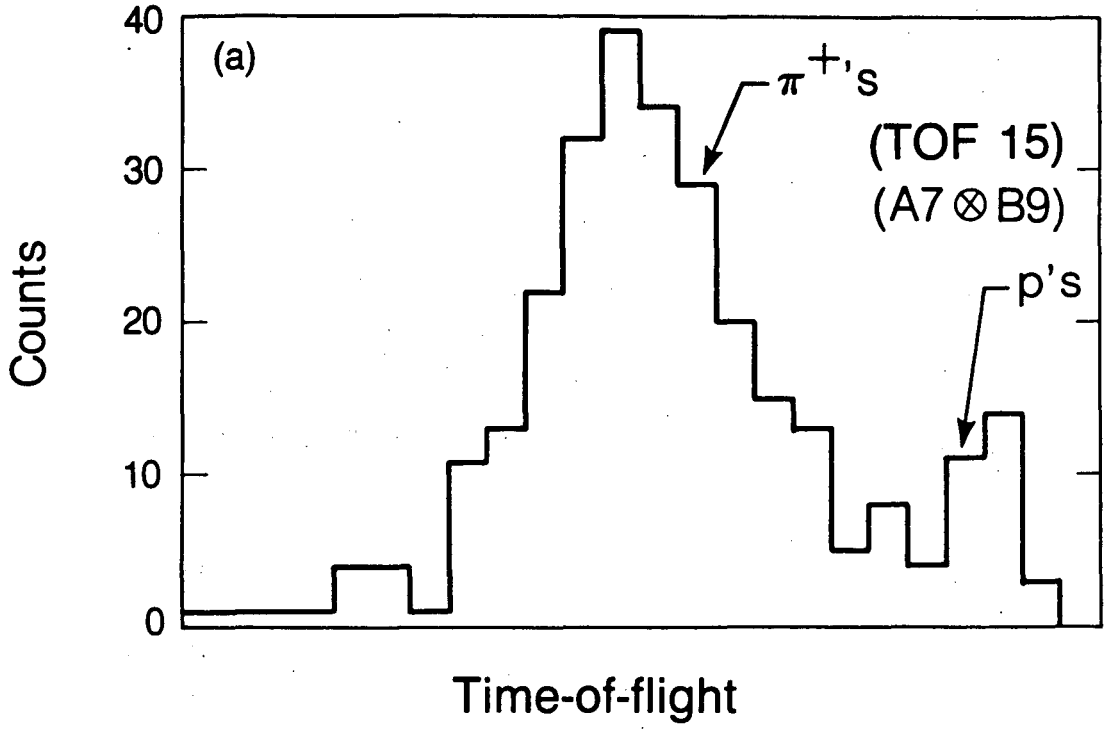

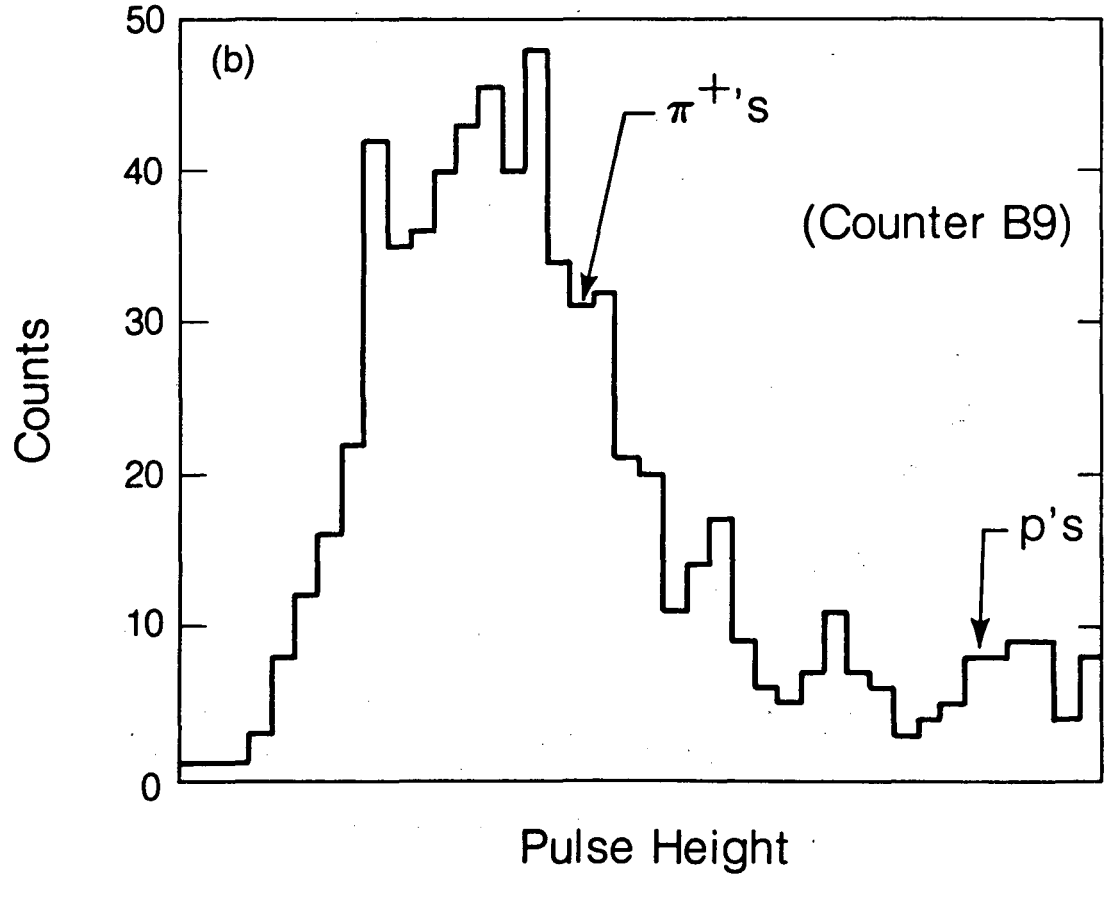

Figure 3 XBL 8311-7322

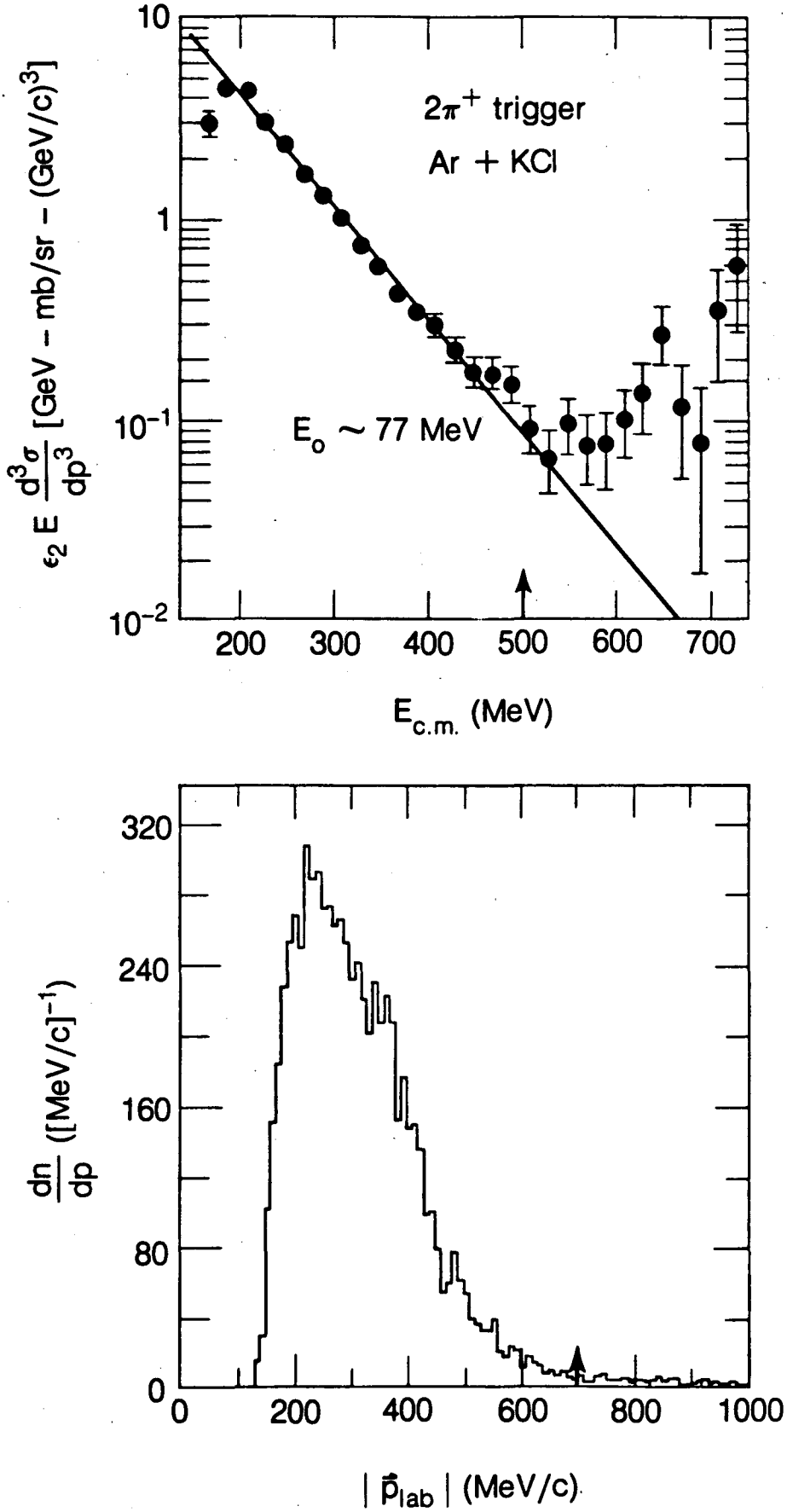

Figure 4

XBL 827-7074

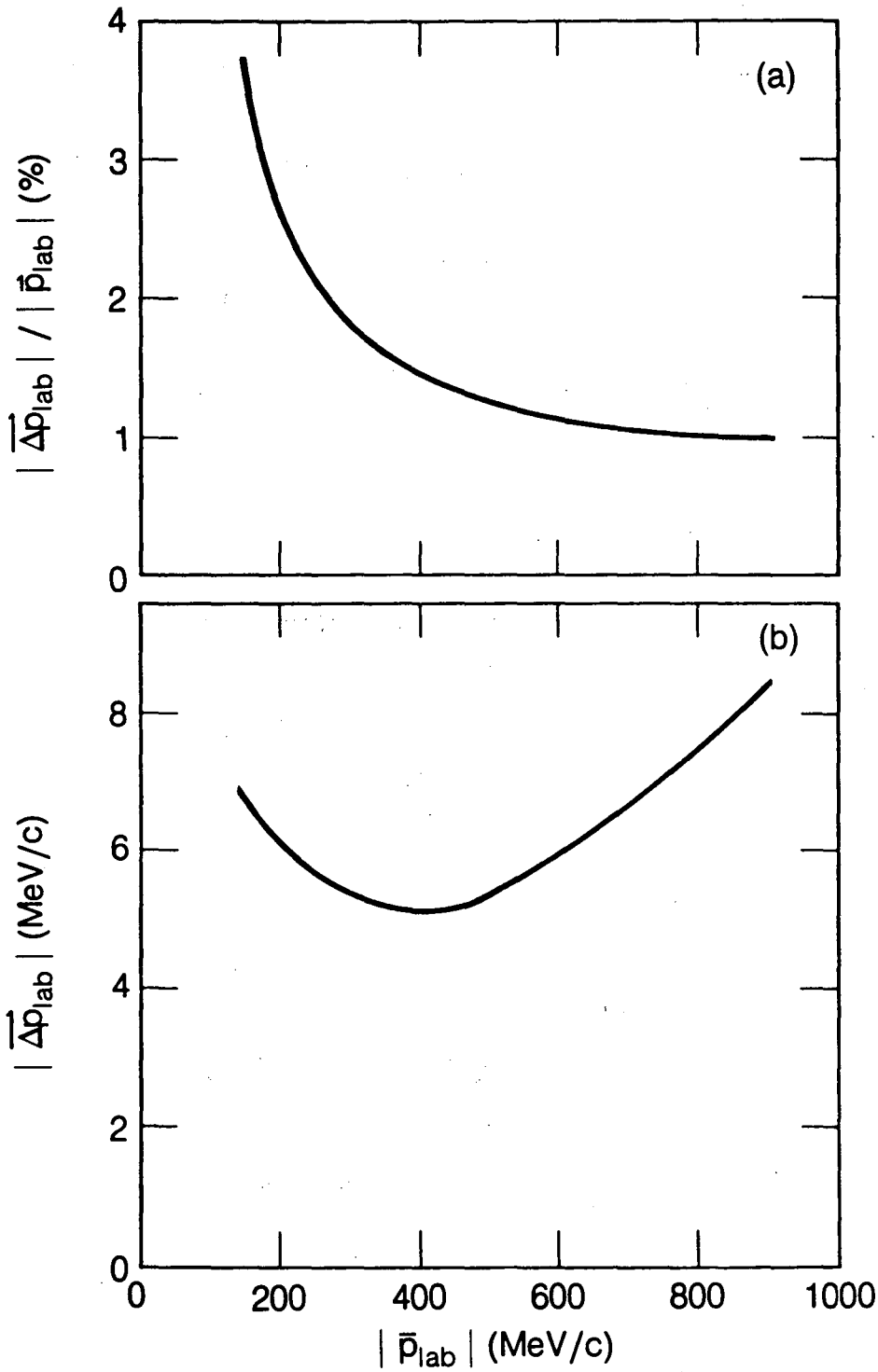

Figure 5

XBL 827-7086

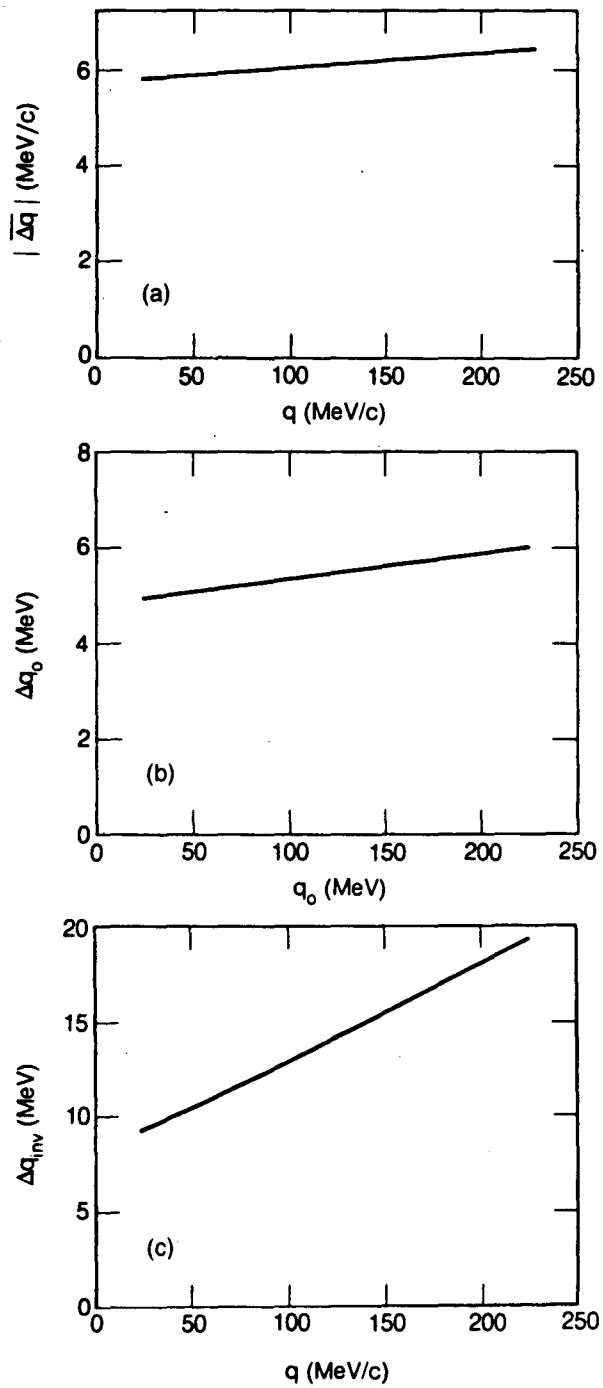

Figure 6 **XBL 8311-7319**

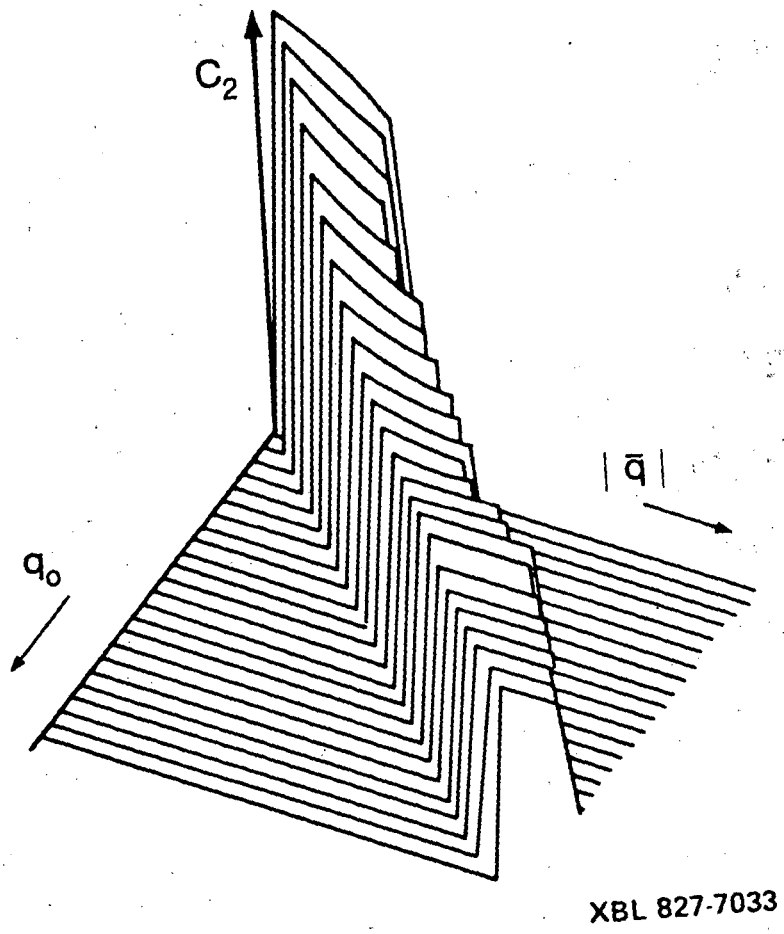

Figure 7

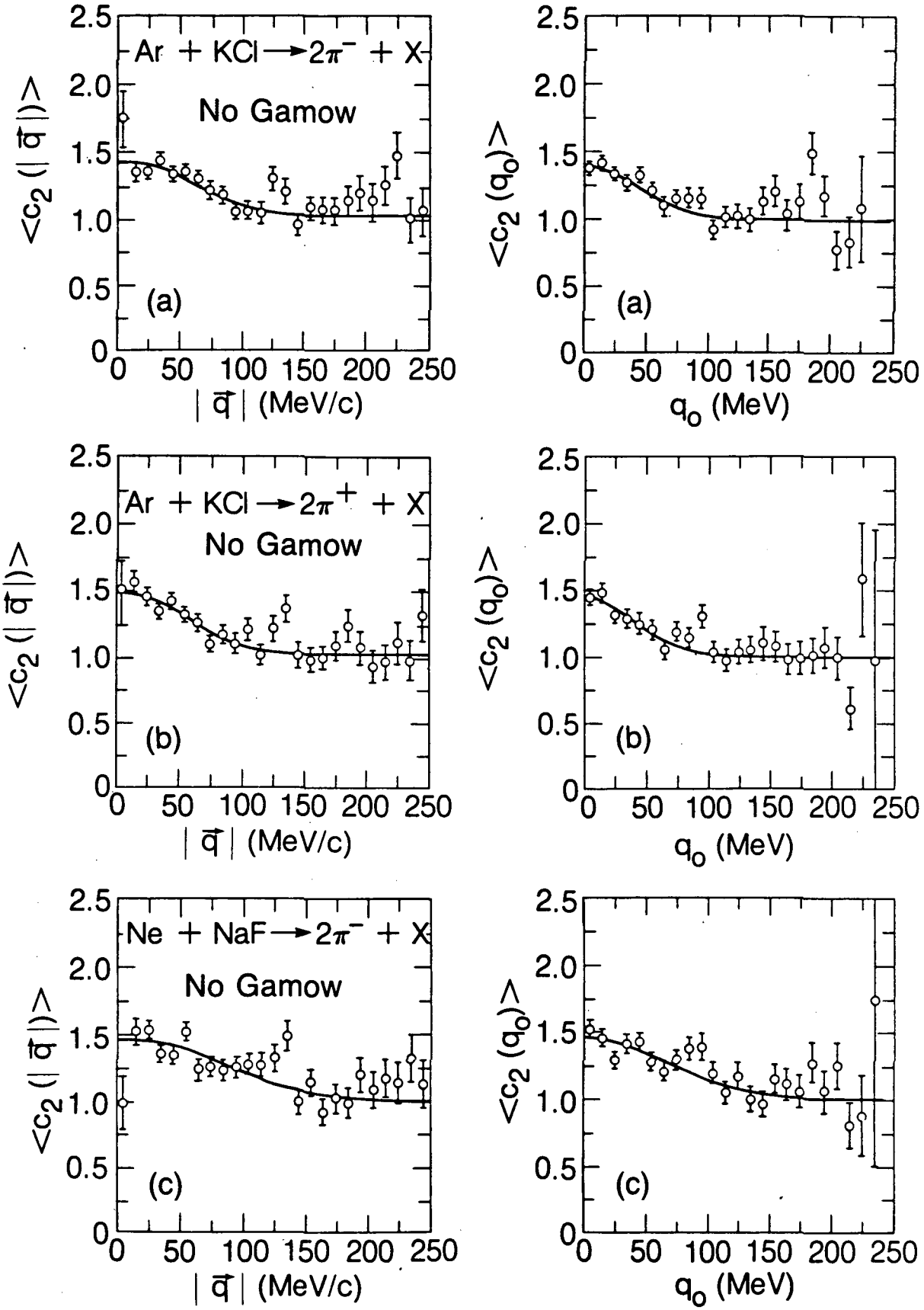

Figure 8

XBL 8311-7320

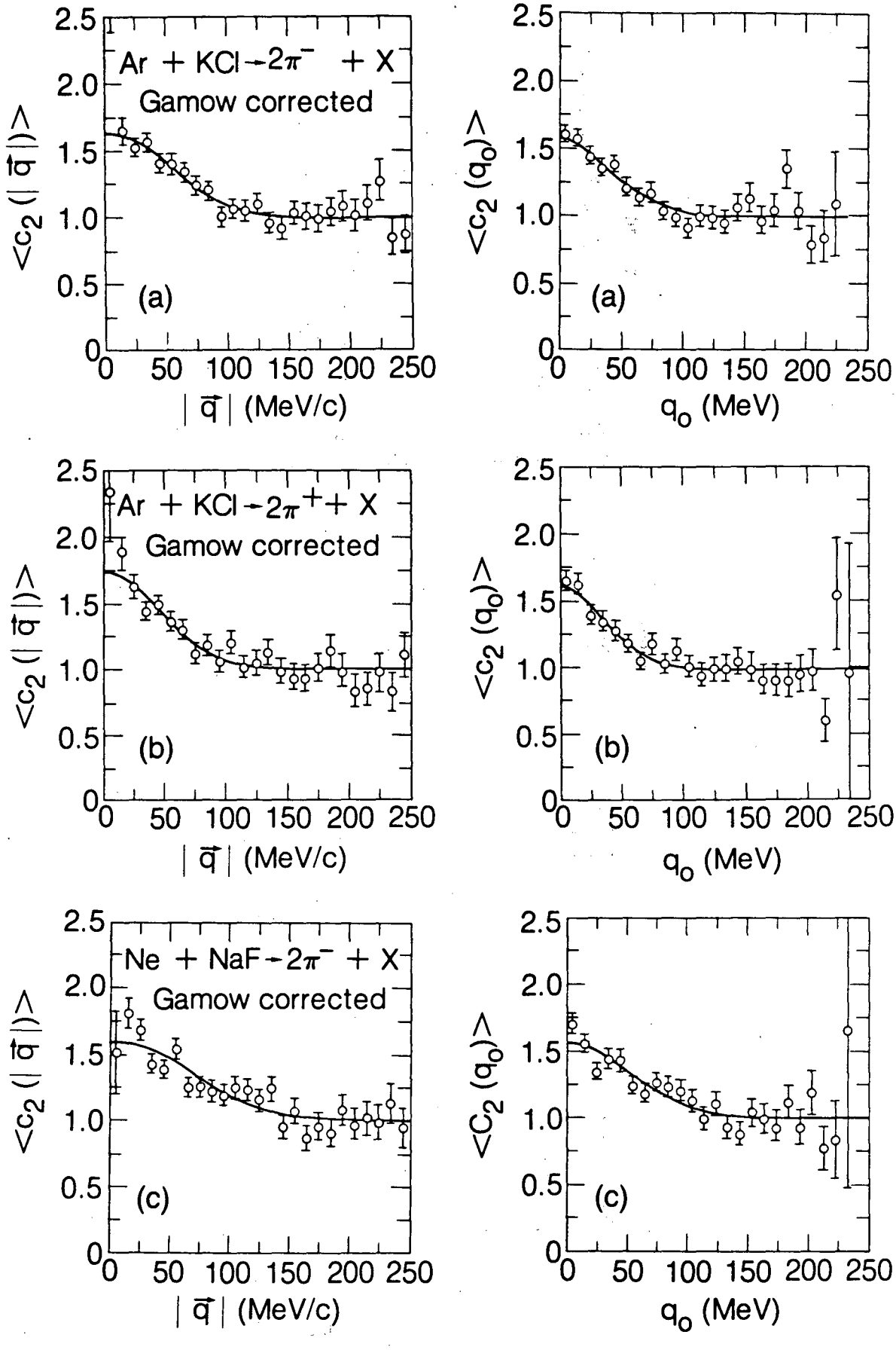

Figure 9

XBL 8311-7321

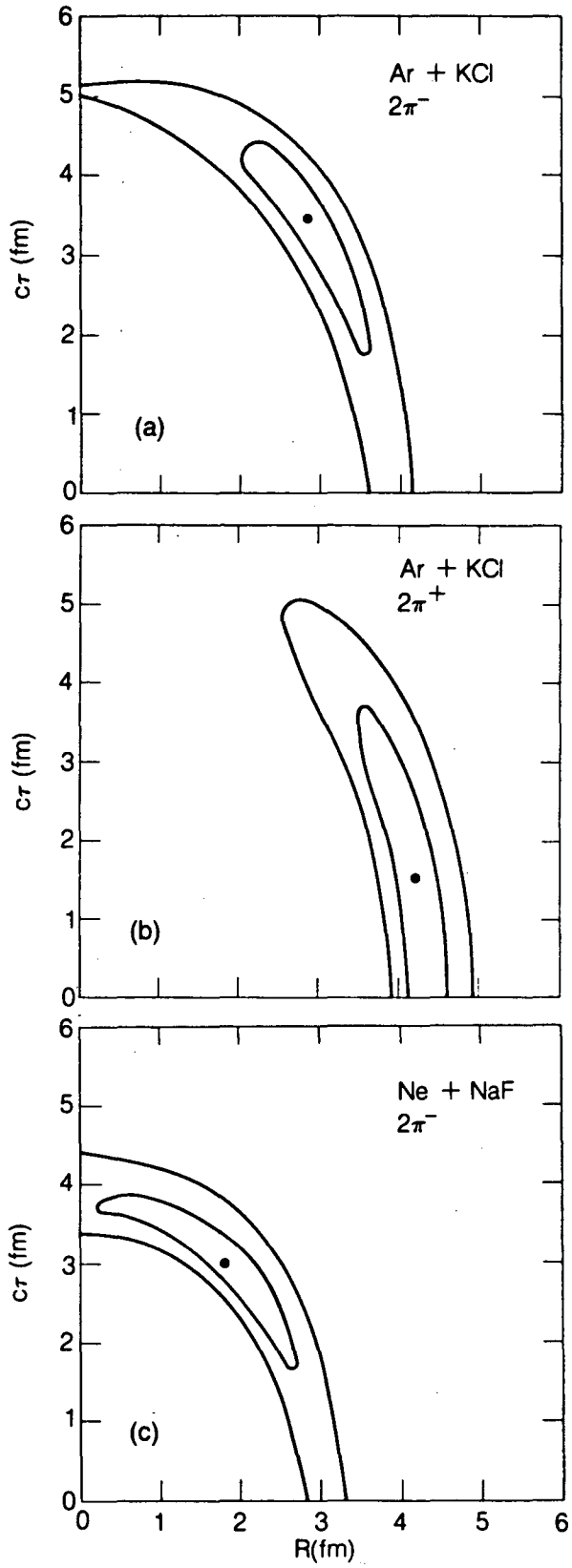

XBL 8311-7318

Figure 10

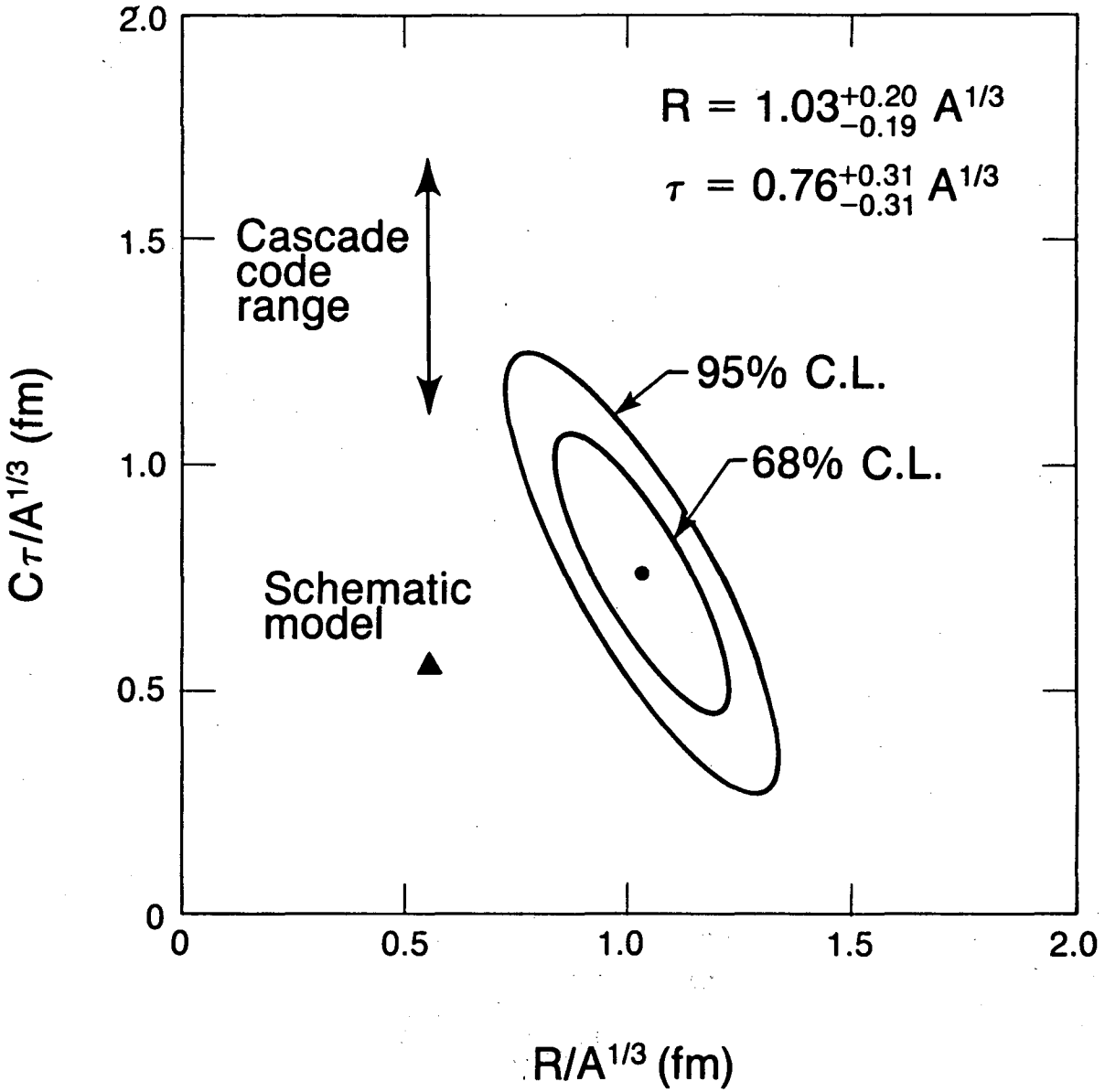

Figure 11

XBL 8312-7487

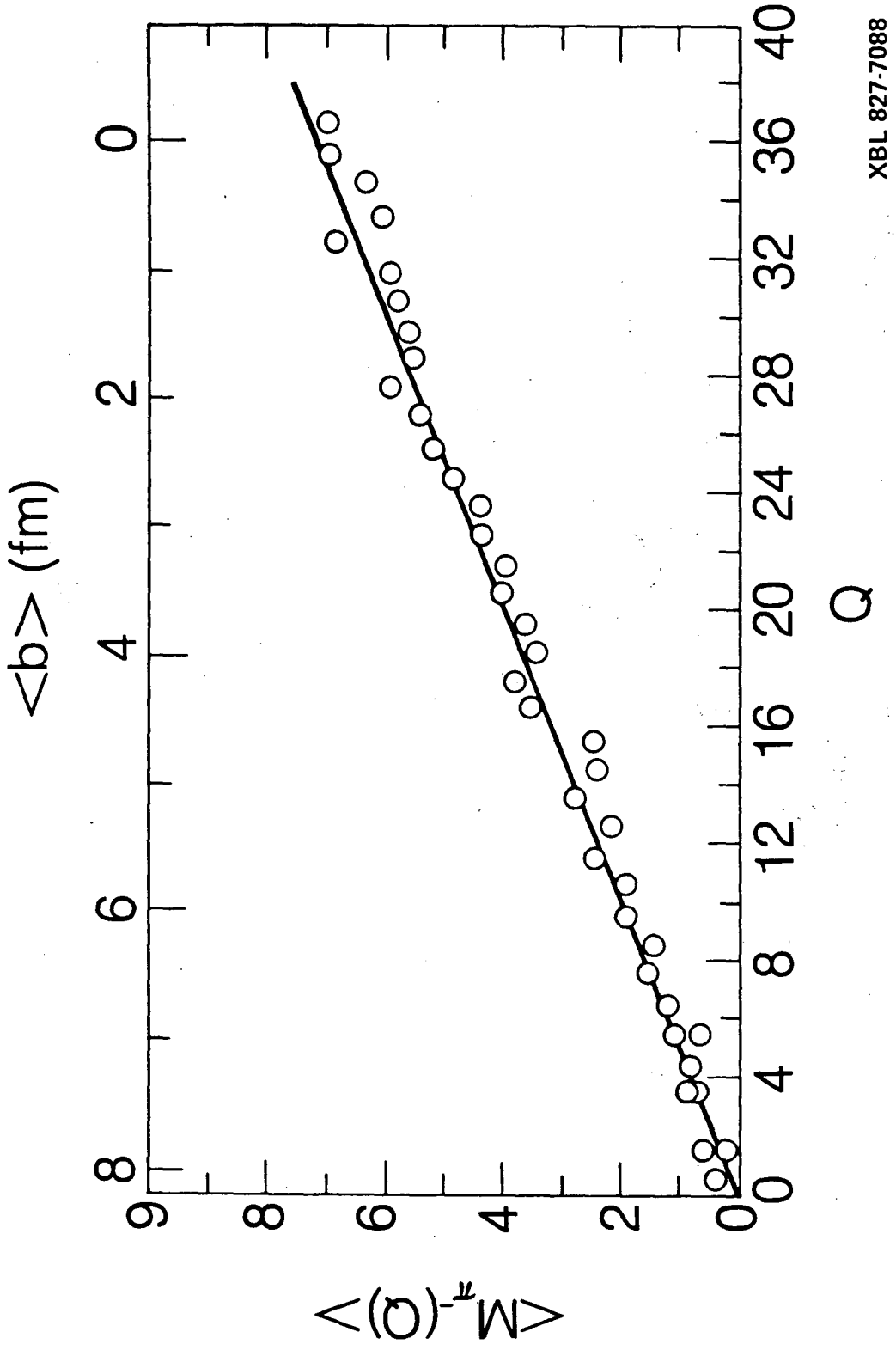

Figure 12

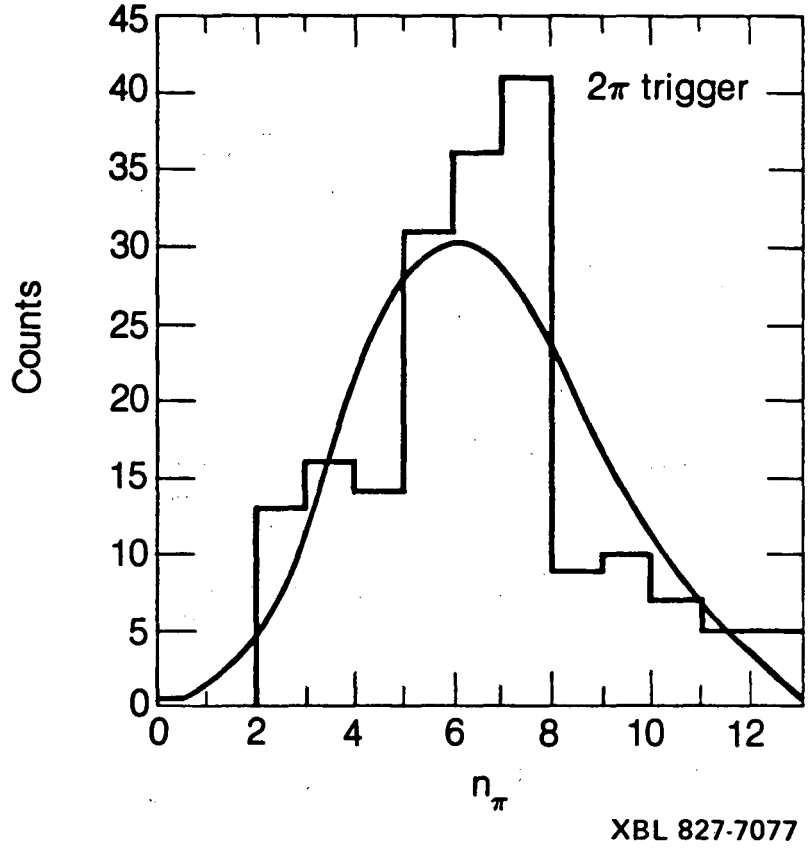
45
40
35
30
25
20
15
10
5
0
Counts
2π trigger
0
2
4
6
8
10
12
n_π
XBL 827-7077

Figure 13

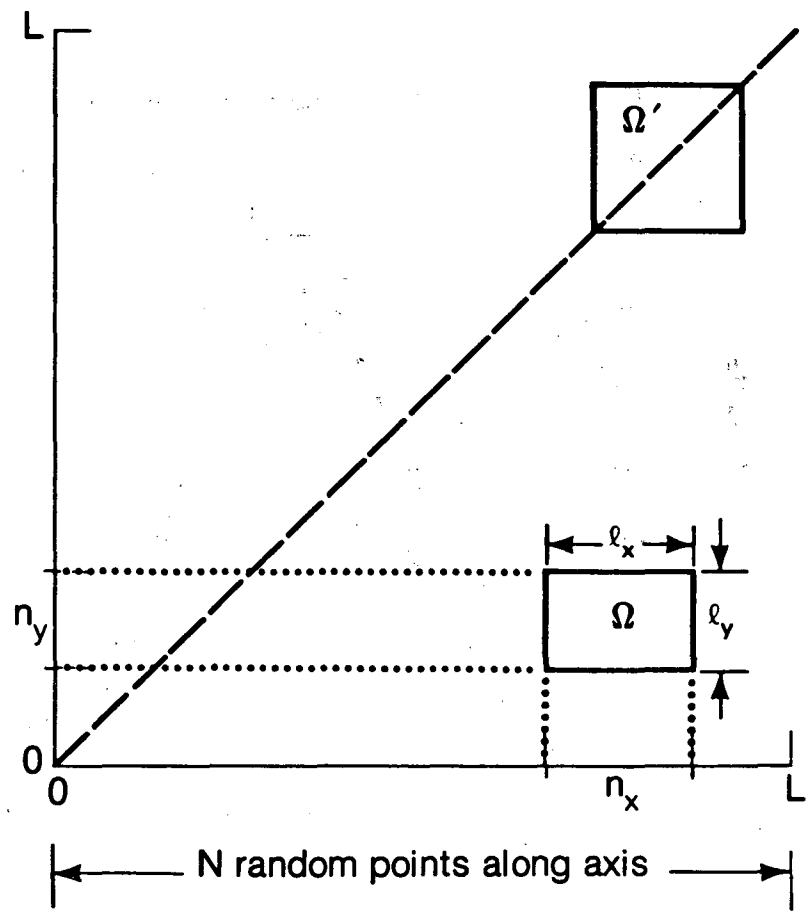

XBL 827-7035

Figure 14

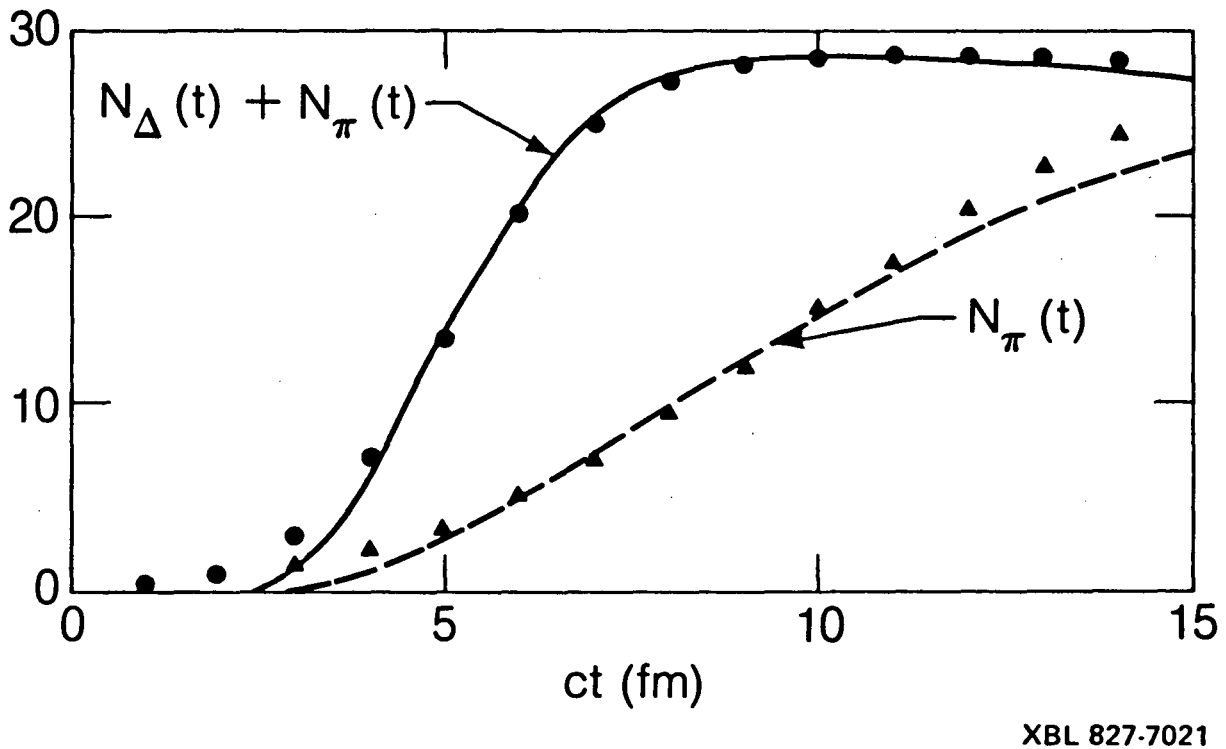

Figure 15

This report was done with support from the Department of Energy. Any conclusions or opinions expressed in this report represent solely those of the author(s) and not necessarily those of The Regents of the University of California, the Lawrence Berkeley Laboratory or the Department of Energy.

Reference to a company or product name does not imply approval or recommendation of the product by the University of California or the U.S. Department of Energy to the exclusion of others that may be suitable.

TECHNICAL INFORMATION DEPARTMENT
LAWRENCE BERKELEY LABORATORY
UNIVERSITY OF CALIFORNIA
BERKELEY, CALIFORNIA 94720